

**CORRELATION PROPERTIES OF DOPPLER FADING IN CELLULAR
NETWORKS IN GHANA**

By

Kusi Ankrah Bonsu B.Sc. Physics (Hons)

KNUST

A Thesis submitted to the Department of Telecommunication Engineering,

Kwame Nkrumah University of Science and Technology

in partial fulfillment of the requirements for the degree of

MASTER OF SCIENCE

Faculty of Electrical and Computer Engineering

College of Engineering

November 2011

DECLARATION

I hereby declare that this submission is my own work towards the partial fulfillment for the award of degree of MSc (Master of Science) in Telecommunication Engineering and that, to the best of my knowledge, it contains no material previously published by another person nor material which has been accepted for the award of any other degree from any University, except where due acknowledgement has been made in the text.

KNUST

Kusi Ankrah BONSU (PG1396907)

(Student)

Signature

Date

Certified by:

Rev Dr. K. J. OPPONG

(Supervisor)

Signature

Date

Certified by:

Dr. P.Y OKYERE

(Head of Dept)

Signature

Date

ABSTRACT

Fading is the most observed and frustrating problem in transmitting and receiving radio signals. Studying the correlation properties of fading helps us to design proper communication systems that are robust to it. In this project, received power signal is obtained by drive-test technique. The data collection is done in an operating frequency of 900MHz and 1800MHz and the environments used for the data collection are urban and suburban. The analysis is done using curve fitting tool and distribution fitting tool in Matlab software 7.5.0 (R2007b). The following fading distributions are used, Rayleigh, Rician, Nakagami-m, Lognormal and Weibull. Weibull fading distribution is found to give the best description of fading experienced in Ghana. On the other hand, Rician distribution, Nakagami-m distribution and lognormal distribution have less agreement with the measured data while Rayleigh fading distribution has much less agreement with measured data. The obtained mean scale parameter and the mean shape parameter in the Weibull distribution for the environment considered are 133.76 and 15.93, respectively. Furthermore, the path loss exponents in the near and far fields are also calculated; and the standard deviation of shadowing falls in the range of 4.368dB to 6.180dB. Last but not least, a clear dependence between the root-mean square (rms) delay spread values of the received power signals and the transmitter-receiver separation distance is observed. Ultimately, the analysis on the large-scale fading tends to describe the terrain profile of the environment and it is dependent on the distance.

DEDICATION

To the almighty God for given me the strength and the brain to complete this thesis.

KNUST



ACKNOWLEDGEMENT

Except the LORD builds the house, they labour in vain who build it; except the Lord guards the city, the watchman stays awake in vain (Psalms 127:1). May His name be praised forever.

This thesis is simply the culmination of a few years of learning. This learning process has been possible thanks to many people that believed in me and kept on teaching me many things about life, about science and engineering. First and Foremost, I thank God for helping me to complete this thesis.

I express my grateful to my supervisor, Rev. Dr. J. K. Opong, for his guidance and encouragements.

I thank Nana Kena Frimpong of Mathematics Department, KNUST,

Dotche K. Agbeblewu, my coursemate for his immense contribution towards this project, monsieur merci beaucoup, Que Dieu te benisse;

Mark Bediako (CSIR) for given me access to Sciencedirect directory to get journals to read for my literature review.

I am expressing my sincere thanks to all faculty members of the Telecommunication Engineering Department of KNUST for their valuable suggestions,

My wife, Mrs. Akua Serwaa Bonsu Ankrah, and my lovely son, Nana Kwaku Bonsu Ankrah for their support.

I am immensely grateful to my family members, particularly to my mother. They have always supported me and taught me the things that matter most in life and Deaconess Margaret Acheampong for always making sure I am always on my toes as well as my colleagues (Teachers at Anglican secondary school, Kumasi) for their support

Last but not least I thank Rev Emmanuel Osei Yeboah of Victory Baptist Church for his prayers and support.

Ultimately, I would like to thank everyone who helped me knowingly and unknowingly.

ABBREVIATIONS LIST

AC: Alternating Current

ANN: Artificial Neural Network

ARQ: Automatic Repeat Request

BS: Base Station

BER: Bit Error Rate

BW: Bandwidth

CDF: Cumulative Distribution Function

dB: Decibel

DC: Direct Current

DPSK: Differential Phase Shift Keying

ERP: Effective Radiated Power

GSM: Global System for Mobile communication

GPS: Global Positioning System

KPI's: Key Performance Indicators

LOS: Line of Sight

LSF: Large Scale Fading

Matlab: Matrix Laboratory

MANET: Mobile Adhoc Network

MCE: Mobile Cellular Environment

MS: Mobile Station

OAT: Over-Air-Test

PDF: Probability Density Function

PLMN: Public Land Mobile Network

QAM: Quadrature Amplitude Modulation

RF: Radio Frequency

KNUST



RMS: Root Mean Square

SD: Standard deviation

SIR: Signal-to-Interference Ratio

SR-ARQ: Selective Repeat Automatic Repeat Request

SSF: Small-Scale Fading

T-R: Transmitter- Receiver

WLAN's: Wireless Local Area Networks

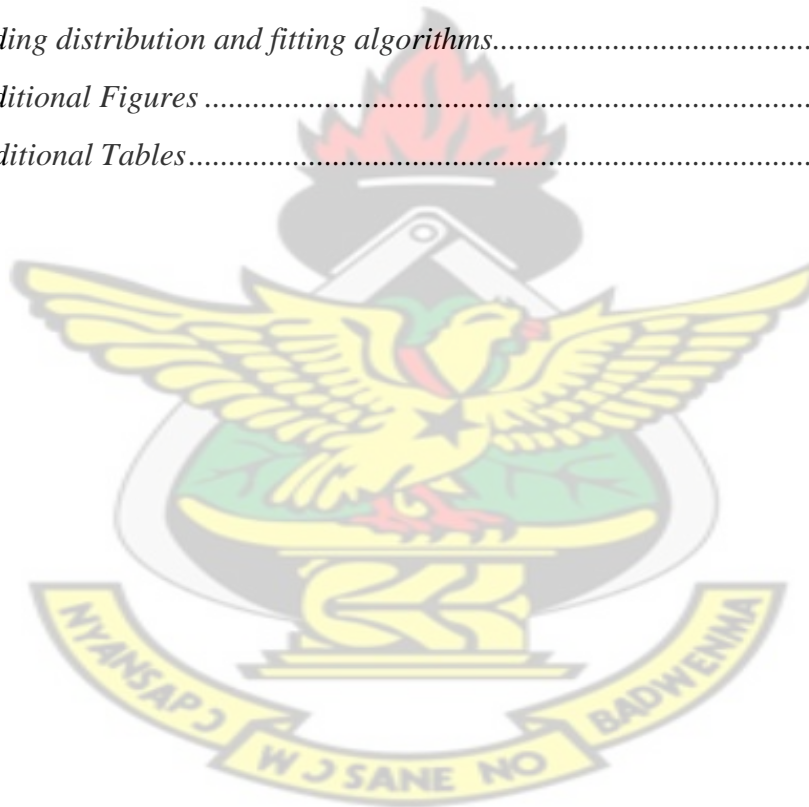
KNUST



TABLE OF CONTENTS

<i>DECLARATION</i>	<i>ii</i>
<i>ABSTRACT</i>	<i>iii</i>
<i>DEDICATION</i>	<i>iv</i>
<i>ACKNOWLEDGEMENT</i>	<i>v</i>
<i>ABBREVIATIONS LIST</i>	<i>vi</i>
<i>TABLE OF CONTENTS</i>	<i>viii</i>
<i>LIST OF FIGURES</i>	<i>x</i>
<i>LIST OF TABLES</i>	<i>xi</i>
<i>CHAPTER ONE: INTRODUCTION</i>	<i>1</i>
1.0 Background	1
1.1 Problem statement.....	2
1.2 Objective	2
1.3. Outline of thesis	3
<i>CHAPTER TWO: LITERATURE REVIEW</i>	<i>5</i>
2.0 Notion of Correlation	5
2.1 Previous related Works	6
2.2. Antenna radiation region.....	10
2.3 Fading.....	12
2.3.1. Multipath fading	13
2.3.2 Types of multipath fading.....	14
2.4. Large-scale fading (LSF)	14
2.5. Small-scale fading (SSF).....	15
2.5.1. Types of small-scale fading (SSF).....	15
2.5.2. Small-scale fading models.....	16
2.5. 3. Mobile multipath channel parameters	20
<i>CHAPTER THREE: METHODOLOGY</i>	<i>25</i>
3.0. Motivation	25
3.1 Research Problem.....	25
3.2. Drive-test.....	26
3.3 Data collection and environment.....	28
3.4 Data sampling size	28

3.5. Data processing	28
<i>CHAPTER FOUR RESULT AND ANALYSIS</i>	29
4.1. Channel characteristics.....	29
4.2. Large-scale fading study in mobile environment.....	32
4.3. Small-scale fading distribution in mobile environment.....	34
4.4. Effect of statistical path loss.....	36
4.5. Shadowing autocorrelation and delay spread properties.....	37
4.6. Delay spread optimization using least square algorithm.....	48
4.7. The Weibull Parameters in Ghana mobile environment.....	50
<i>CHAPTER FIVE: CONCLUSION AND RECOMMENDATIONS</i>	54
<i>REFERENCES</i>	56
<i>Appendix A: Fading distribution and fitting algorithms</i>	61
<i>Appendix B: Additional Figures</i>	63
<i>Appendix C: Additional Tables</i>	68



LIST OF FIGURES

Figure 2. 1: Antenna radiation regions	11
Figure 2. 2: Multipath fading channel.....	13
Figure 3. 1: Drive-test system setup [66].....	26
Figure 3. 2: Interface of devices configuration in TEMS Investigator 6.1.3	27
Figure 4. 1: A set of received power in 50s (stationary mode).....	29
Figure 4. 2 Simulated Rayleigh channel with sampling frequency of 1/1000Hz	30
Figure 4. 3: Simulated Rayleigh fading with sampling frequency of 1/10000Hz	31
Figure 4. 4: Rayleigh and Rician channel comparison	31
Figure 4. 5 Path loss fading comparison.....	32
Figure 4. 6: Large-scale fading model comparison	33
Figure 4. 7: Small scale fading distributions with measured data	34
Figure 4. 8: Fading distribution comparison.....	35
Figure 4. 9: Statistical comparison of path loss	36
Figure 4. 10: Delay spread profile from a fixed transmitter	37
Figure 4. 11: Delay spread profile distribution.....	37
Figure 4. 12: Delay spread profile characteristic	38
Figure 4. 13 Autocorrelation of shadowing in near field (environment B)	40
Figure 4. 14 Autocorrelation of shadowing in far field (environment B).....	41
Figure 4. 15 Autocorrelation of shadowing in near field (environment C)	43
Figure 4. 16: Autocorrelation of shadowing in environment B (Far - field)	44
Figure 4. 17 Autocorrelation of shadowing in environment D (Near - Field).....	45
Figure 4. 18: Autocorrelation of shadowing in environment D (far - field).....	46
Figure 4. 19: Data fitting plot (near field environment D)	47
Figure 4. 20 Data fitting plot (far field environment D).....	48
Figure 4. 21: The theoretical delay spread	49
Figure 4. 22: The optimized delay spread.....	49
Figure 4. 23 Weibull distribution comparisons in different environments.....	50
Figure 4. 24: Optimized Weibull fading model (Env. B)	51
Figure 4. 25: Optimized Weibull fading model (Env. C)	52
Figure 4. 26: Optimized Weibull fading model (Env. D).....	52

LIST OF TABLES

Table 4. 1: Statistics of measured received power in environment B (Near field).....	39
Table 4. 2 Statistics linear fitting (near field environment B)	39
Table 4. 3: Statistics of measured received power in environment B (far field)	40
Table 4. 4 Statistics linear fitting (far field environment B).....	41
Table 4. 5: Statistics on measured received (Rx) power (near field environment C).....	42
Table 4. 6 statistics of measured received power (Far field environment C)	43
Table 4. 7 Statistics of measured received power in the near field (Environment D)	44
Table 4. 8 Statistics of measured received power in the far field (Environment D).....	45
Table 4. 9: Derived of weibull's fading parameters	50



CHAPTER ONE

INTRODUCTION

1.0 Background

In mobile cellular environment (MCE), the receiving antenna may receive a signal from more than one path. This is referred to as multipath signal propagation. This results from the fact that, there are clutter between the receiver and the transmitter (Johnson, 2009). The antenna will combine coherently the signals from the multipath signals. In this case, the amplitudes and relative phases of the multipath signals may differ from one another. The field strength at user end is the phasor sum of all the signals received. In addition, the following factors affect the signal strength at any given location: the transmitter position, height, power, frequency, the topography of the terrain between the transmitter and receiver, the clutter (buildings, trees etc.), and the materials in the immediate location (Daniels, 2010). The medium may exhibit many imperfections in time varying manner as results of multipath fading, interference, Doppler shift, and shadowing (chan, 2010). Multipath propagation means that the received signal consists of components arriving through different paths. Multipath radio signal propagation occurs on all terrestrial radio links. The radio signals not only travel by the direct line of sight path, but also the transmitted signal may leave the transmitting antenna in only the direction of the receiver, but over a range of angles even when a directional antenna is used. As a result, the transmitted signals spread out from the transmitter. The signals may reflect off a variety of surfaces and reach the receiving antenna via paths other than the direct line of sight path (radio-electronic, 2010). Multipath fading occurs in any environment where

there is multipath propagation and there is some movement of elements, within the radio communication system. This may include the radio transmitter or receiver position, or in the elements that give rise to reflections (Rao, 2010). The multipath fading can often be relatively deep i.e. the signals fade completely away, whereas at the other times fading may not cause the signal to fall below a useable strength. The most troublesome and frustrating problem in receiving radio signals is variation in signal strength caused by fading. Fading is the deviation of the attenuation that a carrier-modulated telecommunication signal experiences over a certain propagation media. (wikipedia, 2011).

1.1 Problem statement

The work compares fading models particularly small-scale ones with signal measurements taken in the Ghanaian environment. The study of small-scale fading helps us identify which type of modulation scheme can be used for a particular environment.

1.2 Objective

The objective of this project is to study correlation properties of Doppler fading in the near and far field of a fixed transmitter (base station) and roving user (mobile station) by considering outdoor measurements. The work identifies the relative interference on the roving user or mobile station (MS) signal.

1.3. Outline of thesis

The remaining chapters are organized as follows:

Chapter 2 introduces:

- Correlation: Define correlation and the significance of correlated signals in mobile telecommunications system.
- Previous related works: findings of related researches done by others.
- Antenna radiation regions: Use field strength attenuation as a function of distance to distinction between the three regions and be clear with the region that is useful in wireless communication systems.
- Fading: Definition of fading and its causes.
- Large-scale fading: Definition, its causes and the models used to estimate large-scale fading.
- Small-scale fading: Definition, its causes, types and fading models for small-scale fading and autocorrelation theory;

Chapter 3 illustrates

- The methodology of measuring the received power using the drive-test procedures.
- Data collection: the drive-tests were performed in different CDMA networks for data collection in an operating frequency of 900MHz and 1800MHz.
- Data sampling size: Data capturing size was carried out by drive-test software. It takes 115 measurement points in one minute.

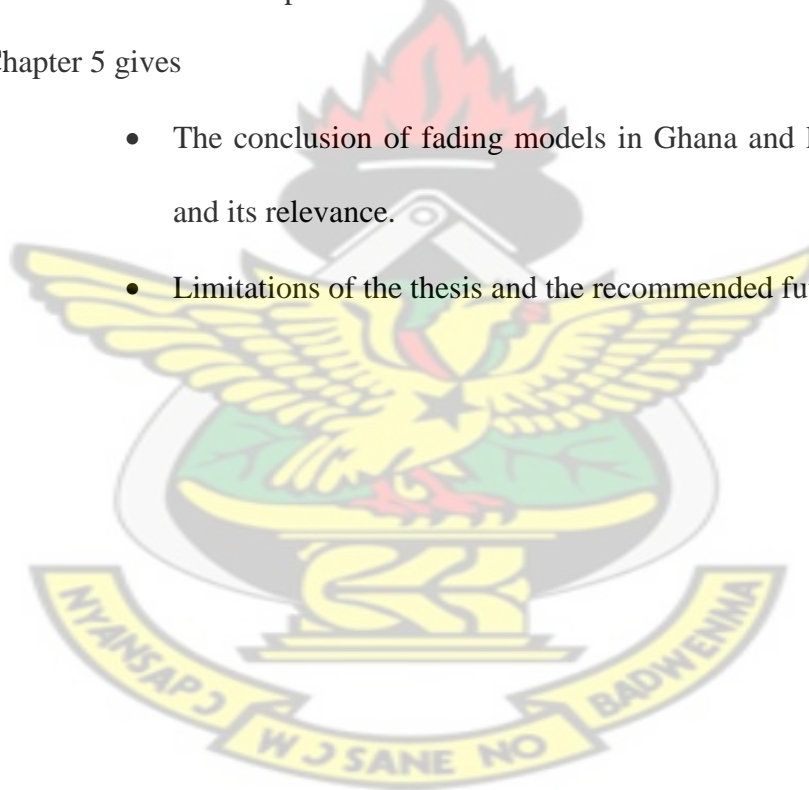
- Data processing: Data was processed in Microsoft excel and then in Matlab 7.5.0 (R2007b) software.

Chapter 4 presents

- The results and a thorough analysis on the results of small-scale fading and large-scale fading.
- Statistics of the various environments, shadowing autocorrelation and the delay spread properties
- Weibull parameters in Ghana.

Chapter 5 gives

- The conclusion of fading models in Ghana and large-scale fading and its relevance.
- Limitations of the thesis and the recommended future works.



CHAPTER TWO

LITERATURE REVIEW

2.0 Notion of Correlation

Correlation is defined as a measure of the relation between two or more variables (Statsoft, 2011). The measurement scales used should be at least interval scales but other correlation coefficients are available to handle other types of data. Correlation coefficients can range from -1 to +1. The value of -1 represents a perfect negative correlation while a value of +1 represents a perfect positive correlation. A value of 0 represents a lack of correlation. It follows that correlation helps us to understand whether the relationship is positive or negative and the strength of the relationship (experiment-resources, 2011).

In mobile telecommunications system, correlated signals received at mobile station from two or more base stations are meant to initiate handover process (Zhang et al, 2008). The mobile unit makes a continuous signal measurement of surrounding base stations. Depending on its velocity, the handover process may also be affected by Doppler shift.

In this chapter, we present a review on previous related works, antenna radiation region, fading, large scale fading, small scale fading and autocorrelation theory.

2.1 Previous related Works

In (Sundstrom, 2006) measurements were conducted on the received power from two GSM900 base stations at various distances and receive antenna elevation. The gain height found was not significant enough to motivate a lot of effort in increasing the antenna elevation for vehicle-mounted antennas; a 1.5dB increase in the signal power was obtained when going from the antenna elevation of 1m to 5m and 2dB when going from 1m to 9m. The distribution of the received signal was also examined and it was found to be hard to do an accurate statement concerning the distribution but Rayleigh distribution was very likely one for both low and high received antenna elevations. In (Krievs, 2004), long – term fading was examined through measurement by Rhode Schwarz drive-test. It was observed that the standard deviation of the received signal level from the measurement (1-3dB) showed little agreement with the theory (6-12dB) in (Sklar, 1997) (Chugg, 1999). In (Jalden et al, 2006) large-scale fading was investigated through indoor measurements at KTH, Stockholm and TUI, IImenau. It was observed that large-scale fading did not depend on the distance between the BS and the MS; but then it was mainly dependent on the environment and the correlated signals could be found when the environment was similar. Moreover in (Hong A,Thomae R.S, 2009) their report indicated that the higher the BS height, the higher the large-scale fading in a particular case study in the near field of the transmitting antenna. It was found that the inter-sector correlation of the large scale parameters was around 0.9 in the overlapped areas. Furthermore a simple autocorrelation model was proposed for the received signal in shadow fading in a mobile radio system (Ohashi M,Shiraki K, 1991). The standard deviation of the signal strength was estimated to be 7.5dB and 4.3dB and correlation at distance of 100m and

10m was estimated to be 0.82 and 0.3 for suburban and urban respectively. The results showed good agreement with the measured data from suburban environments. In microcellular environments the signal envelope was corrupted with multipath fading and the model predictions were less accurate. In (Graziano, 1978), the correlation in shadow fading between MS and two BSs was analyzed and the correlation was found to be around 0.7-0.8 for small angles less than 10^0 (ten degrees) and later (Weitzen J, Lowe T, 2002) argued that the correlation in shadow fading could be less than 0.7 even for small angles. In (Jalden et al, 2005) it was observed that the base station and the mobile station angular spreads were correlated when the BSs were closed. Whereas in (Gudmundson M. , 1997) a simple autocorrelation model for fading in mobile radio channels was proposed. It was observed that the model fitted for both macrocells and microcells and results showed that the model fit was good for macrocells to medium cell sizes but not for microcells. In (Zhang et al, 2008), a spatial autocorrelation model of shadow fading in the urban environment in a typical Chinese city with medium size was investigated and it was revealed that it matched with the level crossing rate theory of Gaussian processes and also provided much better results to the empirical results. In (Zhang et al, 2008), autocorrelation function was calculated, it showed that the radio signal existed in regularity, nonstationarity and nonseasonal in that period and also the degree of autocorrelation could not be eliminated as the order of difference increased. (Xia et al, 1993), showed that outside the cell boundary, the radio signal decreases very rapidly with distance and theoretically it was investigated that vertical polarization had little effect on fading as compared to the horizontal polarization. In (Nam H. , 2008), the root mean square (RMS) delay spread values were found to be between 3 to 23ns and showed a

good normal fit and showed that there was no relation between the RMS delay spread values and the transmitter-receiver (T-R) separation distance. The coherence bandwidths were in the range of 2-180MHz for LOS and 2-24MHz for NLOS. It was observed that the amplitude fading was lognormal over both local and global areas by (Nikookar H, Hashemi H., 2008) and it was shown that people movements could make channel unavailable for about one second (Collonge et al, 2003). In (Athanasiadou et al, 2000), (Ayadi et al, 2005) ray tracing model was used find that typical values of rms delay spread are of the order of microseconds and nanoseconds for outdoor and indoor mobile radio channel, respectively. The same work showed that the mean absolute error is about 4.8dB. The root mean square delay spread was about 10ns for LOS and 32ns and 40ns for NLOS.

Last but not least, In (Rao, 2010), (Yip K.W, Ng T.S, 2000), (Rubio et al., 2007) the technique proposed to model the Nakagami-m fading channel for $0.5 \leq m \leq 1$ yielded good results as compared to the already existing methods and also showed that the special case of $m=1$ was the same as that of Rayleigh PDF. It was observed that the channel simulated could be used to check the performance of the channel. Also the short-term fading conditions of the received envelope in wireless communications channels could be modelled by Nakagami distribution. In (Stefonovic et al, 2007), very important closed-form expressions were obtained for the signal-to-interference ratio (SIR's) probability density function (PDF) and cumulative distribution function. Outage probability, the average output signal to interference ratio (SIR) and the average error probability for coherent and noncoherent modulation were also derived. Selection diversity was an efficient technique that reduces fading and channel interference influence. In (Oestges et

al., 2009), it was observed that for stationary scenarios (both outdoor-to-indoor and indoor-to-indoor) of small scale fading could be well approximated by a Rician or a Nakagami-m distribution and the parameters of these distributions were closely related to the path loss, and possibly, to the distance and for indoor-to-indoor, small-scale fading could also modelled by a single distribution, made up of both Rayleigh and Double – Rayleigh fading and it was observed that the distribution was likely Double-Rayleigh when both the transmitter and the receiver nodes were moving. A large-scale fading correlation was proposed, which enables to relate the correlation to the node mobility. The standard deviation of shadowing in all cases is about 5.85dB. In (Forkel et al, 2008), it was observed that the amplitude fading was lognormal over both local and global areas. Ultimately, in (Tomasevic et al, 2010), a new method for short-term fading simulation using artificial neural network (ANN) was proposed. It was observed that the received signal experienced Rayleigh fading in the chosen environment and could be utilized for practical simulations. In (Ren et al, 2010) and (Stefanovic et al, 2010) infinite-series of expressions for level crossing rate and average fading duration were obtained. It was observed that fading and path loss had an effect on the performance of wireless mobile networks, including wireless local area networks (WLANs) and mobile adhoc networks (MANETs), particularly on the throughputs. In the same work two mathematical expressions of bit error rates (BERs) with Rayleigh fading for differential phase shift keying (DPSK) and quadrature amplitude modulation (QAM) were derived. However, it was found in (vali et al, 2010) that fading had an adverse effect on the acquisition phase performance and could not be fully compensated by increasing the pilot correlation period. It was also observed that the influence of inter-user interference on the acquisition

performance reduces in the presence of fading. In (Xiao et al, 2007), Proposes a cross-layer adaptive transmission scheme, which is an optimum combination of modulation format and packet size, combined with selective-repeat automatic repeat request to improve the throughput in correlated slow-fading channels.

2.2. Antenna radiation region

The antenna radiation region describes the field strength attenuation as function of distance d . The antenna radiation field is divided into three distinct regions illustrated in Figure: 2.1 where the characteristics of the radiated wave are different. While these are not firm boundaries, they represent conventional usage and provide some insight into the actual radiated field as a function of distance from the antenna (antenna-theory, 2011).

In the reactive near-field the equation is given as:

$$d < 0.62 \sqrt{\frac{D^3}{\lambda}} \quad (2.1)$$

where D is the maximum linear dimension of the antenna, and λ is the wavelength.

In the immediate vicinity of the antenna, we have the reactive near field. In this region, the fields are predominately reactive fields, this means that the Electric (E) - and Magnetic (H) - fields are out of phase by 90 degrees to each other. This portion of the antenna field is characterized by standing or stationary waves which stored energy and are harmful to the human body.

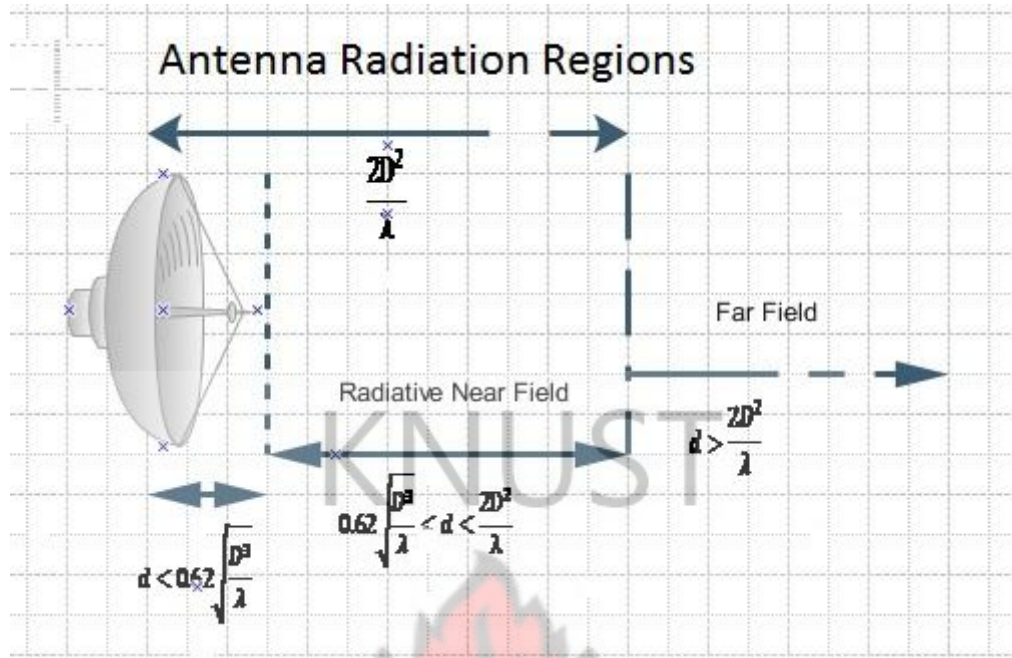


Figure 2. 1: Antenna radiation regions

The radiating near-field or Fresnel region is the region between the reactive near field and the far-field region. This is also called the transition region. The transition region is expressed as in Equation 2.2:

$$0.62 \sqrt{\frac{D^3}{\lambda}} < d < \frac{2D^2}{\lambda} \quad (2.2)$$

In this region, the reactive fields are not dominating. The radiating fields begin to emerge. However, unlike the Far Field region, the shape of the radiation pattern may vary appreciably with distance.

The far field region is the most important region. It is the useful radiation pattern in wireless communication system. This is the region of operation for most antennas (antenna-theory, 2009).

The far-field or Fraunhofer region is defined for distances(d) such that:

$$d > \frac{2D^2}{\lambda} \quad (2.3)$$

In the far-field, the Electric field and Magnetic field are assumed to be orthogonal. This portion of the antenna field is then characterized by radiating or propagating waves which represents transmitted energy and also the field distribution is independent of the distance from the antenna. From the above explanations of antenna radiation regions it follows that fading will be experienced by a mobile station in the far field. This is as results of the obstacles or objects in its surrounding environment. However, the received signal is subject to distortion as a result of fading in the propagation medium. Automobiles and even people will cause reflections. The profile of signal distortion is called fading.

2.3 Fading

In wireless communications, fading is the deviation of the attenuation that a carrier-modulated telecommunication signal experiences over a certain propagation media.

The fading may vary with time, geographical position and/or radio frequency and is often modeled as a random process. A fading channel is a communication channel that experiences fading. In wireless systems fading may either be due to multipath propagation, referred to as multipath induced fading or due to shadowing from obstacles affecting the wave propagation sometimes referred to as shadow fading.

According to (Krievis, 2004), fading in radio interface manifests itself in 3 ways:

- Long-term fading caused by obstacles in signal path (shadowing, diffraction) with period of 10-100 wavelengths with typical variation around the mean of 6-10 dB;

- Short-term or Small-scale fading with rapid signal level changes 20-30dB in small distance less than wavelength or time;
- Random frequency modulation due to varying Doppler shifts.

2.3.1. Multipath fading

Multipath fading is a result of obstruction on a direct wave. In radio communications system the signal will reach the receiver not only through the line-of-sight (LOS) path but also other paths as a result of reflection from objects such as buildings, hills, ground, water etc., that are adjacent to the main path as shown in Figure 2.2.

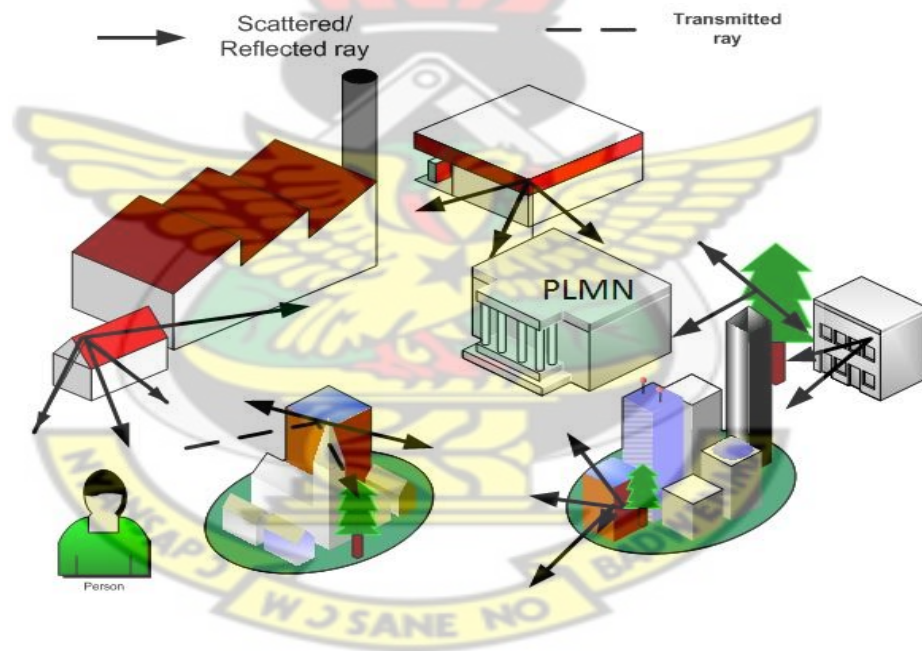


Figure 2. 2: Multipath fading channel

The total signal at radio receiver is the summation of the different signals being received. They all have different path lengths, the signals will add (i.e., constructive) and subtract (i.e., destructive) depending on their relative phases. In most cases there will be changes in the relative path lengths and this could be as a result of either the radio transmitter or

receiver moving or objects moving. This will result in the phases of the signals arriving at the receiver changing and this will in turn result in the signal strength varying as a result of the different way in which the signals sum together and this causes fading that is present on many signals (Goldsmith, 2005).

2.3.2 Types of multi-path fading

Propagation models have traditionally focused on predicting the average received signal strength close spatial proximity to a particular location (Rao, 2010). Multipath fading can be divided into two main classes: large-scale fading and small-scale fading.

2.4. Large-scale fading (LSF)

Large-scale fading is the variation of the mean signal strength over large distances or long time interval (Rappaport et al, 1997). It is mainly due to the absorption of RF energy in the ionosphere and it is found by maintaining the transmitter and receiver fixed while signal absorption occurs due to reflection, diffraction and scattering. Different fading models are developed to estimate large scale fading such as Longley-rice model (Longley & Rice, 1968), Durkin model (Edwards & Durkin, 1969) Okumura model (Okumura et al., 1968), Hata model (Hata, 1980), Walfisch and Bertoni model (Walfisch & Bertoni, 1988) and wideband PCS microcell model (Feuerstein et al, 1994).

2.5. Small-scale fading (SSF)

Small-scale fading is concerned with the rapid fluctuations of the signal over short time periods or over short distances. Multiple versions of the signals arriving at the receiver at different times are subjected to constructive and destructive interference which leads to fading. According to (Rappaport, 1996) , small-scale fading manifests itself in three ways:

- Variation of the signal strength over short distances or short time intervals
- Random frequency modulation on the signal due to Doppler shift and
- Time dispersion (echoes) as result of multipath propagation delay

Small-scale fading occurs in the urban areas due to the height of the mobile antenna which is far below the height of the surrounding buildings. In addition to this, there is no LOS path to the base station. In case where there is LOS, multipath propagation still occurs due to reflection from the ground and buildings. SSF is the most severe problem in the design of mobile communication networks. The physical factors that affect small-scale fading are multipath propagation, speed of the mobile, speed of surrounding objects and the transmission bandwidth of the channel.

2.5.1. Types of small-scale fading (SSF)

Depending on the relation between the signal parameters such as bandwidth, symbols duration and the channel parameters as root mean square delay spread and the Doppler spread, different transmitted signals will undergo different types of fading. There are four types of small-scale fading. They are flat fading, frequency-selective fading, fast fading and slow fading. Small-scale fading, depending on multipath time delay spread, can be

flat fading and frequency-selective. In flat fading the bandwidth (BW) of the signal is less than the coherence bandwidth of the channel. The channel delay spread is less than the symbol duration. This contrasts with frequency-selective fading which occurs when coherence bandwidth falls below signal bandwidth. Moreover, small-scale fading based on Doppler spread can either be fast or slow fading. In fast fading, the Doppler spread time is high, and the coherence time is less than the symbol duration while channel variations are faster than baseband signal variations, The opposite situation results in slow fading (Sklar, 1997).

2.5.2. Small-scale fading models

Small-scale fading occurring in the multipath channel statistically obeys the different characteristics of different random processes such as Rayleigh, Rice, Nakagami-m, etc.

In mobile cellular environments, the Rayleigh distribution is the most popular distribution used to describe the statistical time varying nature of the received envelope of the individual multipath components. Rayleigh model is used when there is no LOS between the transmitter and the receiver (Rao, 2010).

The Rayleigh distribution has a probability density function (PDF)

$$p(r) = \begin{cases} \frac{r}{\sigma^2} e^{-\frac{r^2}{2\sigma^2}}, & (0 \leq r \leq \infty) \\ 0, & (r < 0) \end{cases} \quad (2.4)$$

where σ is the rms value of the received signal before envelope detection and σ^2 is the time-average power of the received signal before envelope detection and the probability that the envelope of the received signal does not exceed a particular value R (the received power threshold), the corresponding CDF is given as in Equation 2.5

$$p(R) = p_r(r \leq R) = \int_0^R p(r)dr = 1 - e^{-\frac{r^2}{2\sigma^2}} \quad (2.5)$$

If the channel is liable to Rayleigh fading, then the mean value r_{mean} of the Rayleigh distribution can be expressed as:

$$r_{mean}=E[r] = \int_0^R r^2 p(r)dr = 1.2533\sigma \quad (2.6)$$

Having a variance given as:

$$\sigma_r^2 = E[r^2] - E^2[r] = \int_0^R r^2 p(r)dr - \frac{\sigma^2\pi}{2}=0.4292\sigma \quad (2.7)$$

The rms value of the envelope is the square root of the mean square and where σ is the standard deviation of the measured received signal to envelope detection. The median value is given by $r_{median}=1.177\sigma$. The mean and median differ by only 0.55dB in a Rayleigh fading signal. Therefore by using the median instead of mean values it is easy to compare different fading distributions.

When the multipath environment of the signal can be characterised by a dominant line of sight, the distribution is described by Rician distribution (Rao, 2010). In Rician distribution, random multipath components arriving at different angles are superimposed on a stationary dominant signal. The PDF of this distribution is given as in (Rao, 2010).

$$P(r) = \left(\frac{r}{\sigma^2}\right)\exp\left(-\frac{r^2+A^2}{2\sigma^2}\right)I_0\left(\frac{Ar}{\sigma^2}\right)u(r) \quad (2.8)$$

Where the parameter A represents the peak amplitude of the dominant signal and I_0 is the modified Bessel function of the first kind and zero order. The Rician distribution is expressed on terms of a parameter K that can be defined as the ratio between the deterministic signal power and the variance of the multipath and it is given by $K = \frac{A^2}{2\sigma^2}$ or

$$\text{in terms of dB } K(dB) = 10\log\left(\frac{A^2}{2\sigma^2}\right)$$

And the parameter K is called the Rician factor and it completely specifies the Rician distribution: as $A \rightarrow 0$, $k \rightarrow -\infty$ dB and as the dominant path decreases in amplitude the Rician distribution degenerates to a Rayleigh distribution.

Nakagami fading is the combination of Rayleigh and Rician fading. The Nakagami fading model was initially proposed because it matched empirical results for short wave ionospheric propagation. Nakagami fading occurs for multipath scattering with relatively large delay-time spreads with different clusters of reflected waves. Within any one cluster, the phases of individual reflected waves are random, but the delay times are approximately equal for all waves (wirelesscommunication, 2011) Rayleigh and Rician fading models have been widely used to simulate small scale fading environments. M Nakagami observed this fact and then formulated a parametric gamma function to describe his large scale experiments on rapid fading in high frequency long distance propagation. The Nakagami distribution or the Nakagami- m distribution is a probability distribution related to the gamma distribution. This more general fading distribution was developed whose parameters can be adjusted to fit a variety of empirical measurements. In (Rubio et al., 2007), the Nakagami probability density function of the received envelope, r also called the m -distribution is given by:

$$p(r) = \frac{2}{\Gamma(m)} \left(\frac{m}{\Omega}\right)^m r^{2m-1} \exp\left(-\frac{m}{\Omega} r^2\right) \quad (2.9)$$

and its k th moment by

$$\mu_k = (r^k) = \int_0^\infty r^k p(r) dr = \frac{\Gamma\left(m + \frac{k}{2}\right)}{\Gamma(m) \left(\frac{m}{\Omega}\right)^{\frac{k}{2}}}$$

Where $\Gamma(\cdot)$ is the gamma function, Ω and m are the parameters of the distribution and where Ω is the average received power and m is the shape factor. The Nakagami distribution includes the Rayleigh distribution for $m=1$ and one-side of the Gaussian distribution for $m=\frac{1}{2}$. When m approaches infinity, it implies that there is no fading (Baltizis, 2010) (Simon & Alouini, 2005).

Weibull fading is a simple statistical model of fading used in wireless communications and based on the Weibull distribution, empirical studies have shown it to be effective model in both indoor and outdoor environments Weibull distribution also represents another generalization of the Rayleigh distribution (Belloni, 2004). A particular class of Weibull distributions was presented by (Sagais et al, 2004).

The probability density function of a Weibull random variable X is given as in Equation 2.10.

$$f(x, a, b) = \begin{cases} \frac{b}{a} \left(\frac{x}{a}\right)^{b-1} e^{-\left(\frac{x}{a}\right)^b}, & x \geq 0 \\ 0, & x < 0 \end{cases} \quad (2.10)$$

where $b > 0$ is the shape parameter and $a > 0$ is the scale parameter of the distribution. Its complementary cumulative distribution function is a stretched exponential function. The Weibull distribution is related to a number of other probability distributions; in particular, it interpolates between the exponential distribution ($b = 1$) and the Rayleigh distribution ($b = 2$) (wikipedia, 2011). On one hand, these fading models find their application in the estimation of the loss deviation also known as shadow fading margin (Shepherd, 1977). The fade margin loss for a given measurement of received signal is given as:

$$F_{loss} = \frac{1.884(d_1 - d_2)}{\ln \ln(Rx_1^{-1}) - \ln \ln(Rx_2^{-1})} \quad (2.11)$$

The shadow fade margin can also be evaluated as in Equation 2.12, through signal measurement.

$$Fade_{margin} = Rx_{level} - Rx_{threshold} \quad (2.12)$$

On the other hand, these fading models are encompassed in the log-distance scale of the path loss model. The resultant path loss (PL_{al}) being a function of **large scale fading** LSF, **small scale fading** SSF (Parsons, 1992) and the **distance in km (d)** between the Transmitter (Tx) and the Receiver (Rx) is given as in Equation 2.13. This path loss model is also known as the statistical model of path loss.

$$PL_{al} = LSF[dB] + SSF[dB] + 10 \log_{10}(d[km]) \quad (2.13)$$

where,

$$LSF = |mean(P_{Meas})|$$

$$SSF = std(P_{Meas})$$

and P_{Meas} is the calculated path loss relative to the measured received power.

2.5. 3. Mobile multipath channel parameters

In mobile communication, the experience of echoes at user end at times may also be attributed to the delay spread (Parsons, 1992) of the radio signal. The delay spread is a result of multipath propagation in the radio signal (Parsons, 1992). It is formulated as a mathematical exponential decay. In order to compare different multipath channels and to

develop some design methods for mobile communication systems, different parameters which describe the channel are used. We can define these channel parameters with aid of power delay profile of the channel. Power delay profiles are generally represented as plots of received power as a function of excess delay with respect to a fixed time delay reference. The parameters can be grouped into two categories. They are time and frequency dispersion parameters.

Under time dispersion, the following parameters are considered. They are mean excess delay, root mean square (rms) delay spread, maximum excess delay, coherence bandwidth and out of these the first three parameters are time domain parameters whereas the last one is the frequency domain parameter. It can be found with the aid of spectral response of the channel.

The mean excess delay ($\bar{\tau}$); is the first moment of the power delay profile $p(\tau_k)$ and is defined as:

$$\bar{\tau} = \frac{\sum_k a_k^2 \tau_k}{\sum_k a_k^2} = \frac{\sum_k \tau_k p(\tau_k)}{\sum_k p(\tau_k)} \quad (2.14)$$

RMS delay spread (σ_τ), is the square root of the second central moment of the power delay profile and it is given by

$$\sigma_\tau = \sqrt{\overline{\tau^2} - (\bar{\tau})^2} \quad (2.15)$$

$$\text{where } \overline{\tau^2} = \frac{\sum_k a_k^2 \tau_k^2}{\sum_k a_k^2} = \frac{\sum_k p(\tau_k) \tau_k^2}{\sum_k p(\tau_k)}$$

These two parameters are measured relative to the first detectable signal arriving at the receiver at $\tau_o = 0$. These are defined from a single power delay profile which is temporal

or spatial average of consecutive impulse response measurements collected and averaged over a local area (Rappaport et al, 1997). In (Bultitude et al, 1988) their investigation has revealed that, for 910MHz, RMS delay spread of microcell channel computed with significant multipath components having power level greater than -25dB with respect to the peak can be reduced by a factor of 4 as compared with the macrocell channels. The delay spread in mobile environment is due to the high height of the transmitting antenna and the large size of the macrocell. In the case of macrocell, the excess delay of significant multipath component is evaluated up to 10 μ s (Cox, 1973). In (Hashemi ,K ; Tholl, D, 1994) relation between the delay spread and path loss was also observed in the microcell measurements with low antennas ranging from 3 to 13 m. An upper bound of the delay spread (σ_d) root mean square (RMS) was evaluated as a function of path loss in and it is expressed as:

$$\sigma_d = \exp([0.065 * PL_{Loss}]) \quad (2.16)$$

where σ_d is the RMS delay spread in nanoseconds. In the case of macrocell measurement most papers reported this quantity in microseconds as in (Smith et al, 1998) and PL_{Loss} is the path loss in dB.

In a practical mobile cellular environment, by then the measured received signal power (ΔRx) at an MS is obtained as in **Equation:**

$$\Delta Rx(dBm) = ERP + G_{Rx} - P_{Meas}(dB) \quad (2.17)$$

It comes out that the measured path loss is a function of distance and it is written as follows:

$$P_{Meas}(d) = ERP + G_{Rx} - P_{Rx}(d) \quad (2.18)$$

Taking the absolute derivative of both sides,

$$\frac{\partial P_{L_{Meas.at}}(d)}{\partial d} = \frac{\partial (ERP + G_{Rx} - P_{Rx}(d))}{\partial d} \quad (2.19)$$

It is comes that:

$$\Delta P_{Meas}(d) = \Delta Rx(d) \quad (2.20)$$

ΔRx is the relative variation observed in the received signal

ΔP_{Meas} is the relative variation observed in the path loss signal

It comes that the received signal autocorrelation can be seen as independent of the distance and given as follows:

$$R_{x_k} = \frac{\sum_{i=1}^{N-k} (Rx_i - \overline{Rx})(Rx_{i+k} - \overline{Rx})}{\sum_{i=1}^N (Rx_i - \overline{Rx})^2}$$

For two different positions of the mobile user within the same environment, the shadow autocorrelation relation to the standard deviation of the received signal power is as in (Gudmundson M. , 1991), (Santucci & Granziosi, 2004) and by Equation 2.21.

$$E[Rx_i, Rx_i - \Delta Rx] = \sigma^2 * \exp\left(-\frac{|\Delta Rx|}{\Delta d}\right) \quad (2.21)$$

Where Δd is the relative variation of the distance, and the observed delay spread ($\sigma_d(d)$) is therefore seen as a function of the variation in received signal, and σ the standard deviation of the received power.

Hence it comes out that ($\sigma_d(d)$) is as in Equation 2.22

$$\sigma_d(d) = \exp k * |\Delta Rx(d)| \quad (2.22)$$

This can be written as in Equation 2.23:

$$\sigma_d(d) = 1 + k. Rx(d) \quad (2.23)$$

with k cell size configuration dependency factor.

The value for k in Equation 2.16 is 0.065 for microcell configuration. In the following sections of this thesis, we will derive the value for k in case of macrocell, while considering the received power measurement.

KNUST



CHAPTER THREE

METHODOLOGY

3.0. Motivation

A number of studies have been conducted in the research field of correlation properties of Doppler fading in investigating large-scale fading and small-scale fading. These researches aimed to seek the observed shadowing envelope around the mean path loss. Signal measurement also conducted in these areas, showed that Doppler fading effects are much related to user mobility. However, studying the correlation effect with regard to clutter effect of transmitters has not been researched well. In this project, the interest focuses on transmitters clutter effect while studying the correlation properties of Doppler fading effect on received signals. In this chapter, we present the steps of carrying out the Doppler fading effect in relationship to the distance separation between a moving user and a fixed transmitter is presented.

3.1 Research Problem

The work intends to quantify Doppler fading in mobile cellular environment. The study compares fading models. The thesis also investigates the theoretical delay spread in microcell with measured data obtained from base station in macrocell environment and improve its parameters using the received power signal.

3.2. Drive-test

The measurement procedure is based on the use of a drive test system. A drive-test means drive and test while roaming in the wireless network in a car. The performance of a network especially in terms of RF coverage can be obtained and well explained by this technique. Investigating the RF coverage the following key performance indicators such as the forward transmit power, the down-link transmit and the pilot power strength are obtained. It is recommended that before proceeding on drive test evaluation, the Base Stations (BS) must be identified and then the route to be followed traced. The drive test system measurement tools used are: A Global Positioning System (GPS) receiver antenna, two mobile handsets, drive test software (TEMS investigator 6.1), a laptop, map information software (Map Info 6), inverter, extension board and GPS 76 software version 2 and dc connector source (Battery). The setup of the measurement procedure is illustrated in **Figure 3.1**:

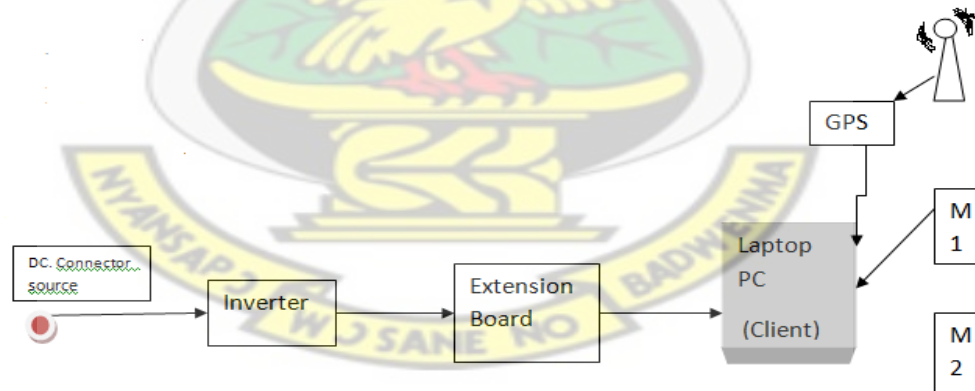


Figure 3. 1: Drive-test system setup (Dotche, 2011)

The inverter in **Figure 3.1** is used, to convert the direct current (DC) voltage at the output of the connector to alternating current (AC). This is used to supply sufficient power to the laptop during a whole day drive test. For a few minutes' drive-testing, the inverter may not be necessary.

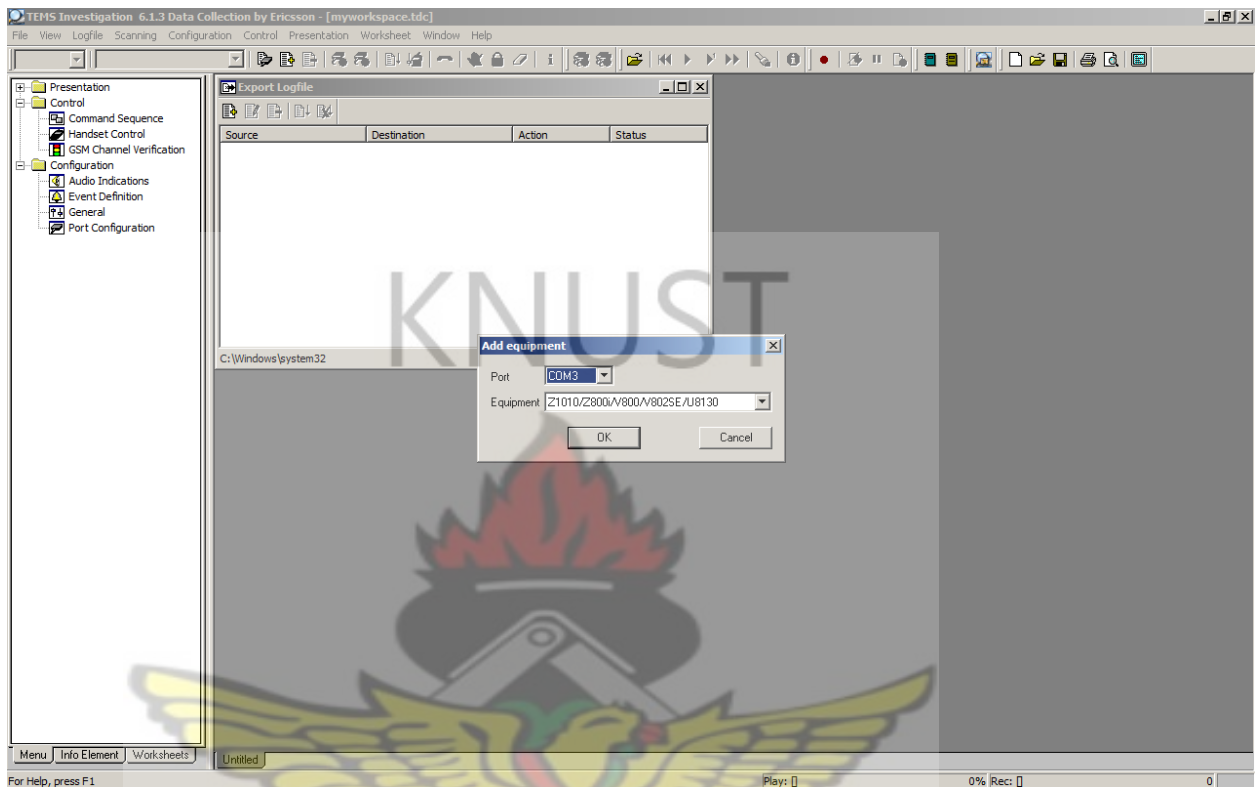


Figure 3. 2: Interface of devices configuration in TEMS Investigator 6.1.3

The outdoor dongle is connected to one COM3 port. The Mobile Equipment line (M1) (COM4 port) will be calling the Mobile Equipment line (M2). In some case, the line (M2) can be on office fixed phone. In this case, one mobile may be used for the drive test or over-air-test (OAT).

The GPS cable is connected on COM6 port.

In this measurement setup, the continuous call (long communication) mode is used for the monitored software during the drive-test. In this mode, the handset makes a continuous call without the user having to redial when the call reception fails. This mode is also known as dedicated mode.

3.3 Data collection and environment

Drive-test was conducted on a network in an operating frequency of 900MHz and 1800MHz providing EVDO-Revision B. In this measurement, communication network terminal was used. The communication network terminal was connected to a laptop monitored by a drive-test software TEMS 6.1 which was a planning and optimization software. These software provide real time information of the network. The environments considered are urban and suburban. The environments A, B, C, D, E represent the following locations in Greater Accra: urban (Accra central market (Makola), Asylum down) and suburban (Legon, Madina and Adenta) respectively. The data was collected in a harmattan season and it was within the period of November 2010 to February 2011.

3.4 Data sampling size

Data capturing size was carried out by the drive-test software. It takes 115 measurements points in one minute. Collected data was processed with the help of a communication network analyzer (CAN) software to spreadsheet.

Some set of samples over a distance of 50m and 100m for the received power have been considered for the near field studies and as well as for the far field studies respectively. In this project distances less than or equal to 300m is considered as the near field and distances greater than 300m is considered as far field.

3.5. Data processing

Data was processed in Microsoft excel and then in Matlab 7.5.0 (R2007b) software.

CHAPTER FOUR

RESULTS AND ANALYSIS

This chapter presents result of the investigation on fading distribution in cellular environment. The analysis is done by means of histograms and plots of the theoretical distribution and the measured data obtained from drive-test system.

4.1. Channel characteristics

Figure 4.1 illustrates a sample of received power against time. A sample of measured received power is considered for 50s in a stationary mode of the user. The frequency, transmitting power (ERP) and the distance between the receiver and the transmitter are 900MHz, 62dB and 50m respectively in environment C.

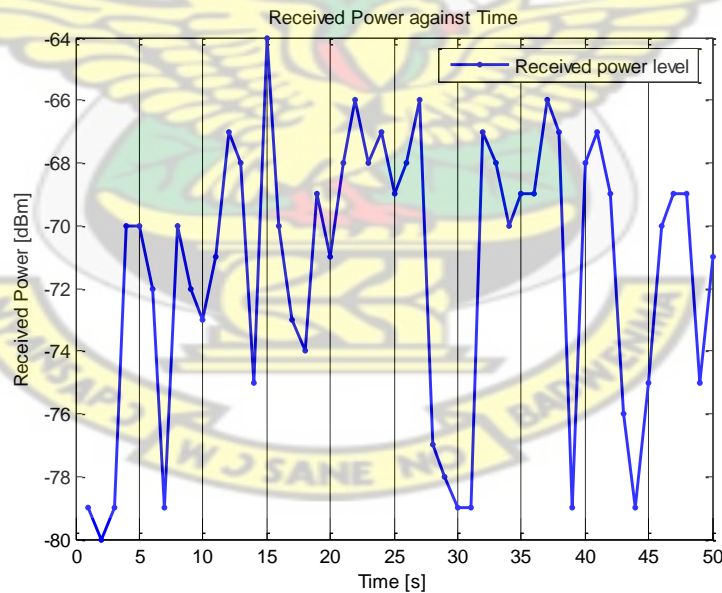


Figure 4. 1: A set of received power in 50s (stationary mode)

In Figure 4.1 a rapid variation of the received signal is observed in a stationary mode. In Figure 4.2 and Figure 4.3 simulated Rayleigh channels (the plots show the magnitude

against the time in ms) are presented with a sampling frequency of 1/1000Hz and 1/10000Hz, respectively whereas the maximum Doppler shift of 50Hz and 100Hz are being considered.

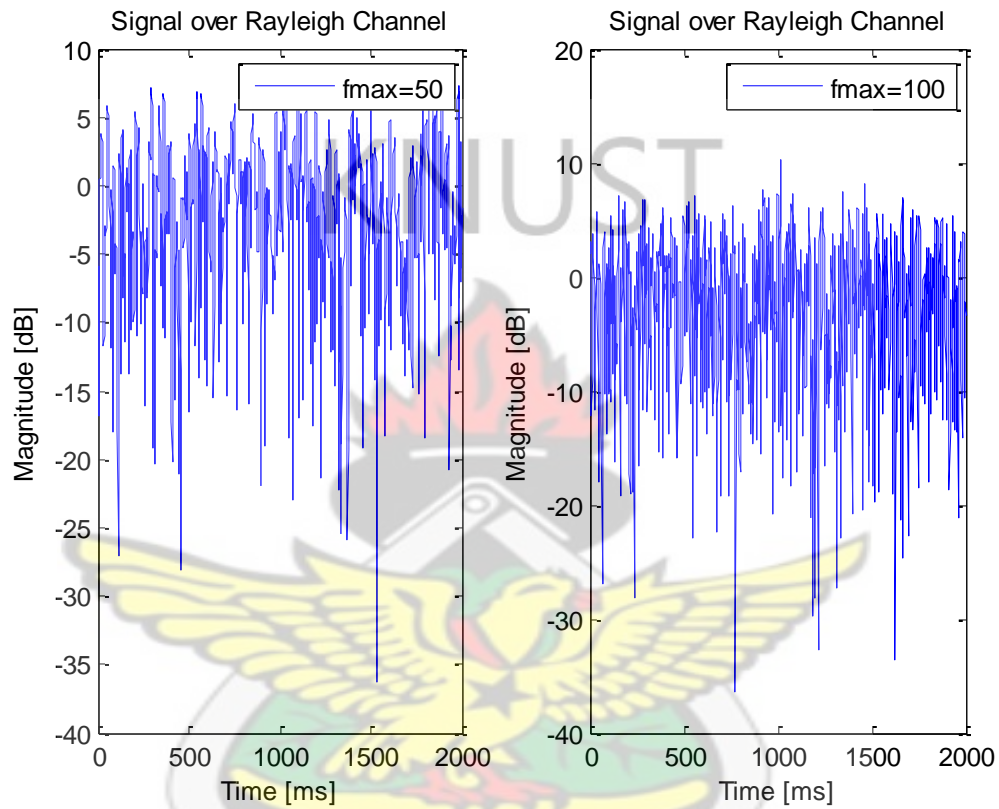


Figure 4. 2 Simulated Rayleigh channel with sampling frequency of 1/1000Hz

In Figure 4.3 and Figure 4.4, for a maximum Doppler shift frequency of 50Hz, the received power signal tends to spread out. However, at 100Hz the received power signal tends to be compact or compressed.

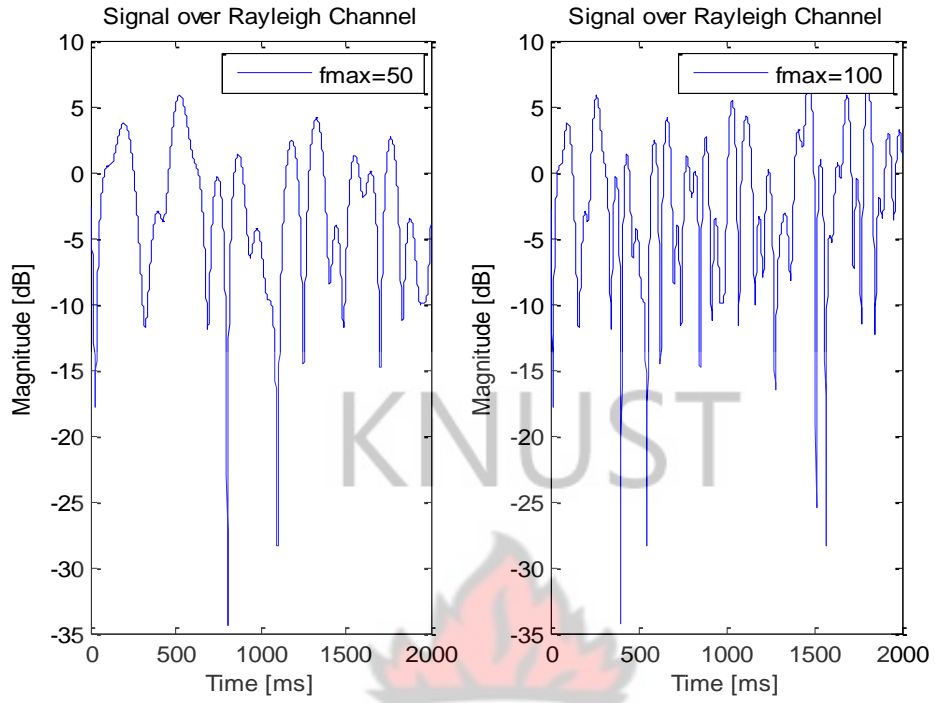


Figure 4. 3: Simulated Rayleigh fading with sampling frequency of 1/10000Hz

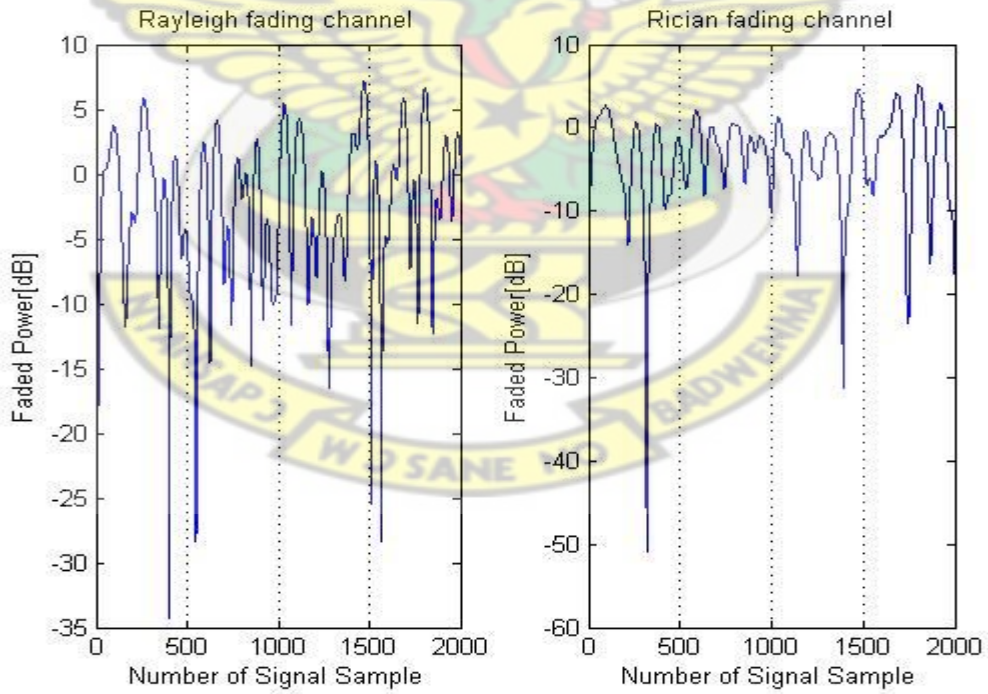


Figure 4. 4: Rayleigh and Rician channel comparison

Figure 4.2 and Figure 4.3 show simulated Rayleigh channel using Matlab software. The Figure 4.4 shows deeper fading depth in Rayleigh than Rician channels. It is also observed that there is no dominant signal and that the channel may follow Rayleigh fading distribution. This may correspond to Nakagami-m fading distribution with a value of $m=1$ in the simulation work of (Rao, 2010).

4.2. Large-scale fading study in mobile environment

The large-scale fading is seen to be the mean around the lognormal fading as shown in blue solid colour. The straight solid line is shown the lognormal fading. The fast fading is displayed the envelope as the measure of dispersion around the large-scale fading.

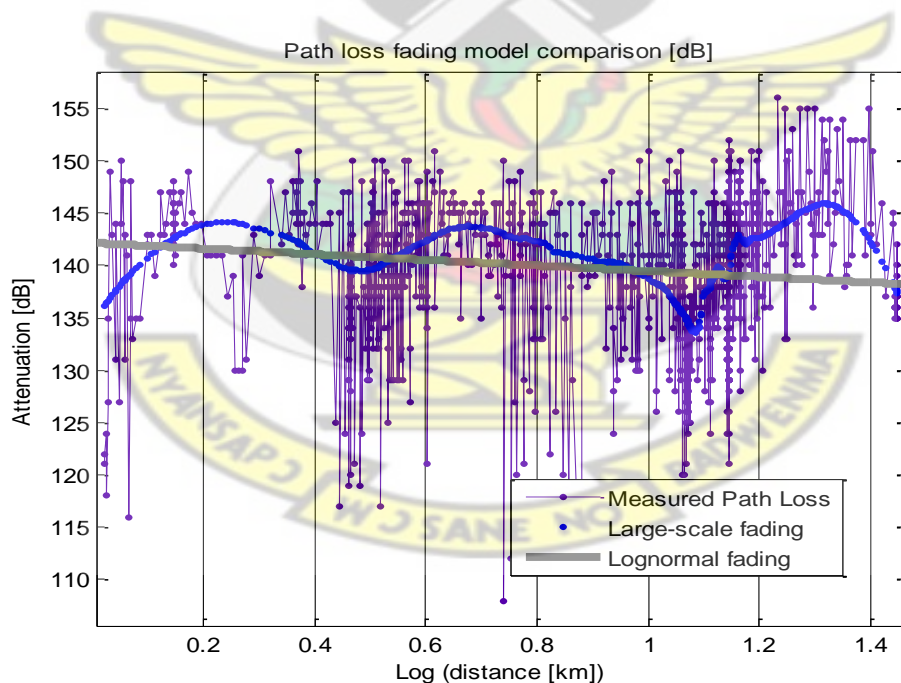


Figure 4. 5 Path loss fading comparison

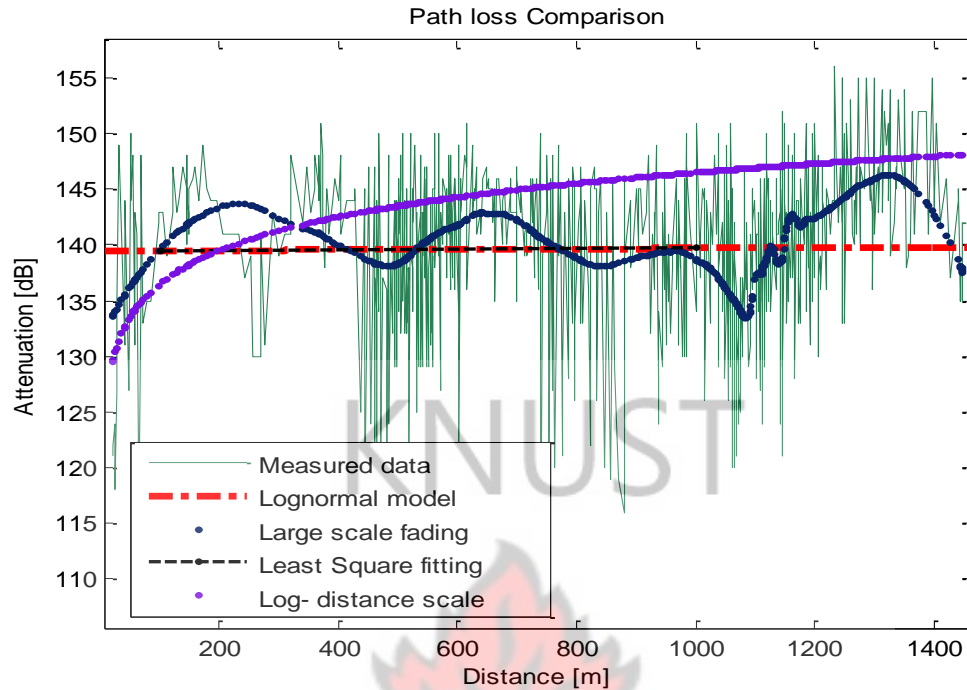


Figure 4. 6: Large-scale fading model comparison

Large-scale fading is obtained by using Robust loess quadratic algorithm in Matlab software. The best fit is shown with measured data, in Figure 4.5 and 4.6; the large-scale fading describes the terrain profile and does depend on the distance. However in (Jalden et al, 2006) with indoor measurements, the large-scale fading was observed not to be dependent on the distance. The shadow lognormal loss tends to be linear. In this particular case, its trend is decreasing explaining that at the far end, the buildings are not much cluttered. Therefore the clutter is less and not much congested. However, the lognormal loss prediction gives a little agreement with the experienced fading. The log-distance model of the path loss also tends to increase faster as compared to the measured data.

4.3. Small-scale fading distribution in mobile environment

The analysis in Figure 4.7, presents a comparative result on small-scale fading distribution with the measured data given in a histogram. The analysis is on the definition of the experienced fading in the environment of Asylum Down area, environment **B**. A distribution fitting tool in Matlab Software is used. The Weibull distribution gives better agreement with the measured data and Rician distribution gives a close agreement with the measured data. Lognormal distribution is observed to be closer to the Nakagami-m distribution.

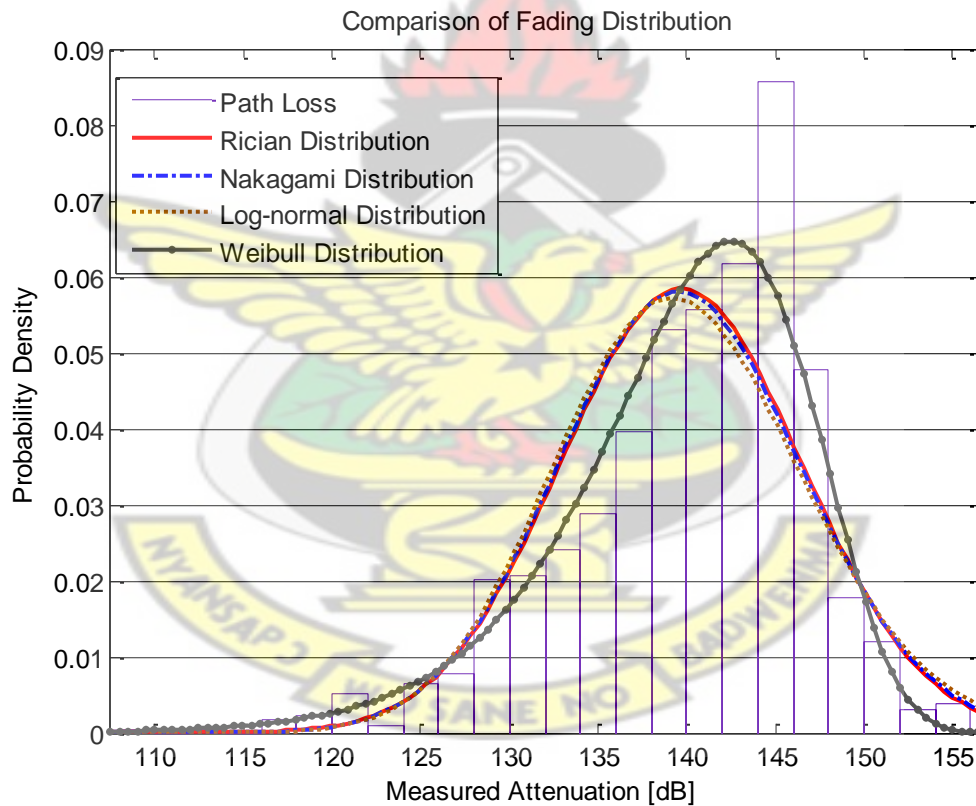


Figure 4. 7: Small scale fading distributions with measured data

However, one may agree with the result that, the prediction of small-scale fading is a Weibull fading distribution with a factor $b=2$ rather than the factor $b=1$ which tends to quantify Rayleigh fading. It shows that the small-scale fading in mobile cellular

environment may not always be attributed to Rayleigh fading distribution. This result differs from the most observed results; it may be explained by the sunny weather and the density of construction materials in Ghana.

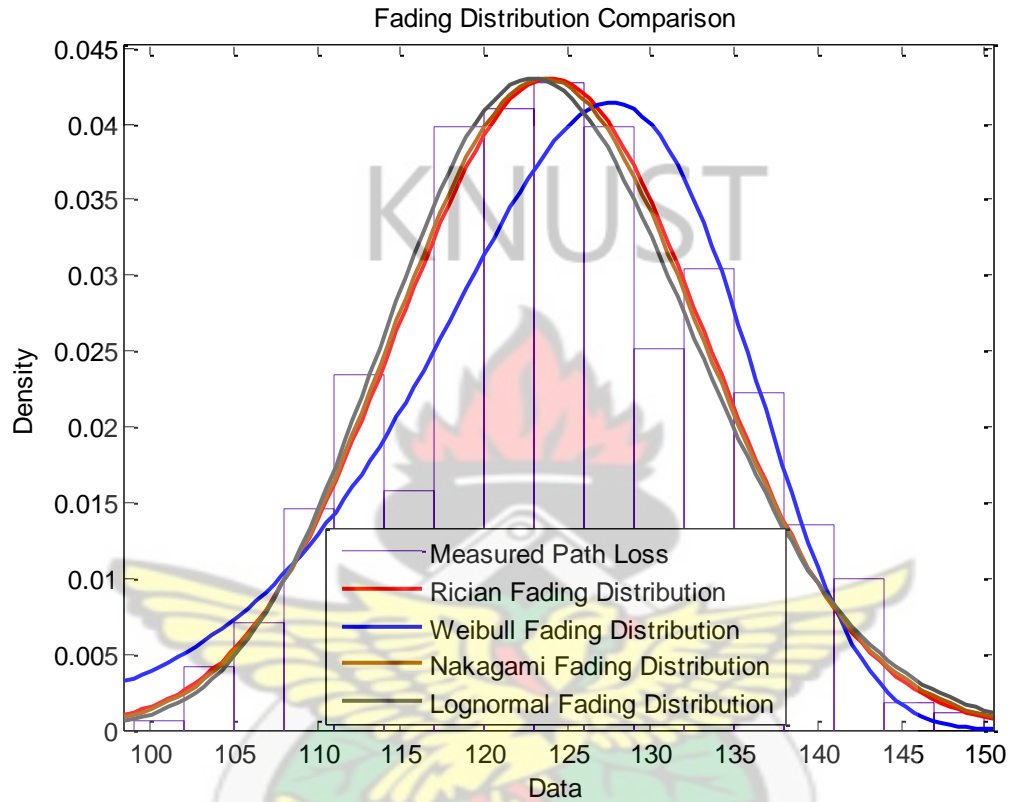


Figure 4. 8: Fading distribution comparison

The Figure 4.8 gives a comparative analysis of Rician, Nakagami-m, lognormal fading and Weibull distribution with the measured data. In the study area of Accra central market(Makola), the Rician, Nakagami-m and lognormal distribution give good agreement with data but the Weibull distribution gives little agreement. The quantified shadow loss distribution may therefore be said to follow a lognormal distribution.

4.4. Effect of statistical path loss

In Figure 4.9, a comparison between a mean path loss and a median path loss is shown.

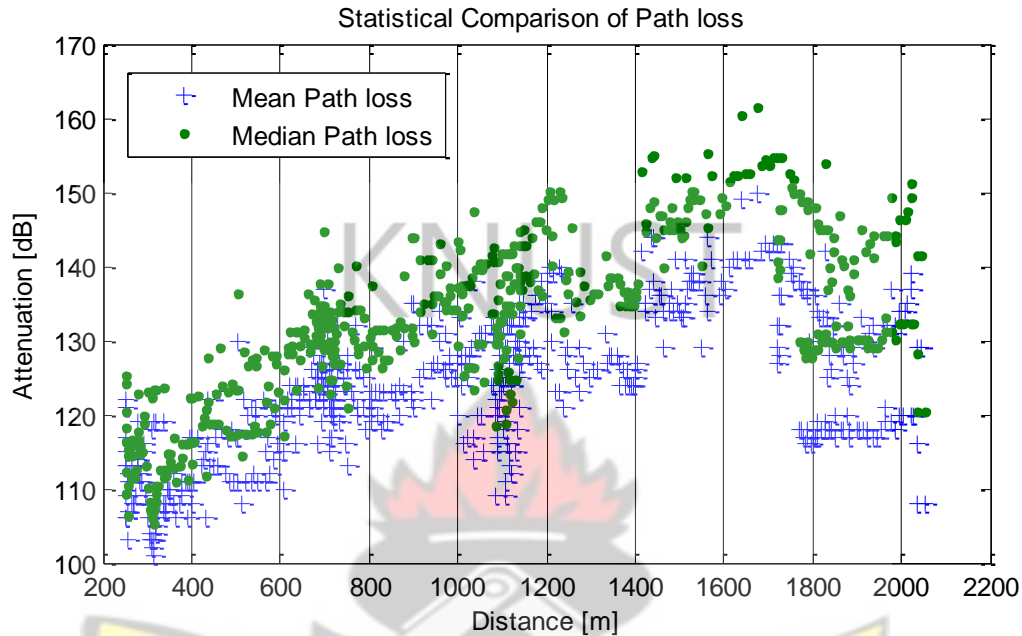


Figure 4. 9: Statistical comparison of path loss

Path loss statistical comparison between the mean and median path loss is presented in Figure 4.9. It is observed that both statistical methods respond to terrain changes, and that the median path loss gives a higher prediction than the mean path loss. The corresponding delay spread is shown in Figure 4.10.

By using the median values instead of the mean values, it is easy to compare different fading distributions as in (Rao, 2010).

4.5. Shadowing autocorrelation and delay spread properties

In Figure 4.10 - 11, the delay spread on shadowing of the mobile environment analysis is presented.

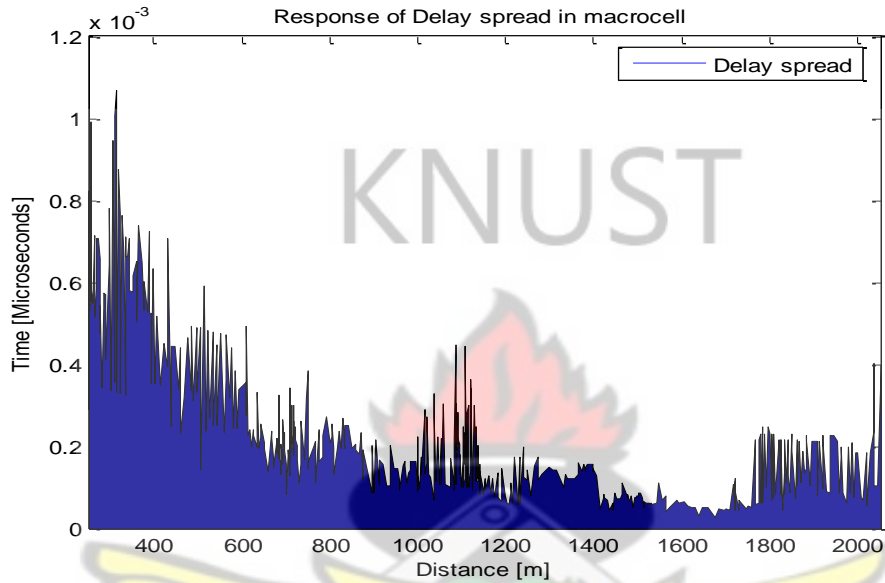


Figure 4. 10: Delay spread profile from a fixed transmitter

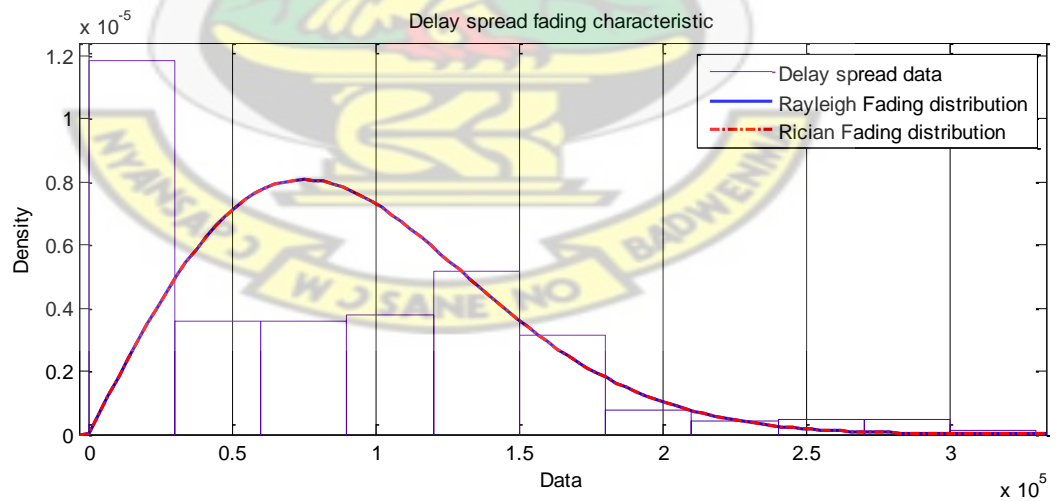


Figure 4. 11: Delay spread profile distribution

In Figure 4.10, it is observed that the delay spread is high at close distance separation of the BS. It decreases as the MS move far away from the BS as observed by (Hashemi ,K ; Tholl, D, 1994) using indoor measurements. However in (Nam H. , 2008) it is observed that the rms delay spread values are not dependent on the transmitter and receiver separation distance, using indoor measurements. This can be explained by the high interference in the near field of antenna located on the sharing mast. Particularly, a poor received power may be experienced by users if the antenna down-tilt is poorly oriented as in (Dotche, 2011) where a drive test measurement was considered. This may unfortunately introduce a long time delay in the call setup. It may be argued that the long delay observed in the near field of the antenna is a result of a poor radio parameters' configuration. On the other hand, the delay spread in macrocell may not be described as Rician or Rayleigh distribution as shown in Figures 4. 12 and Figure 4.13.

In Figure 4.12, the lognormal, Weibull, Nakagami fading distributions give better agreement with the measured data.

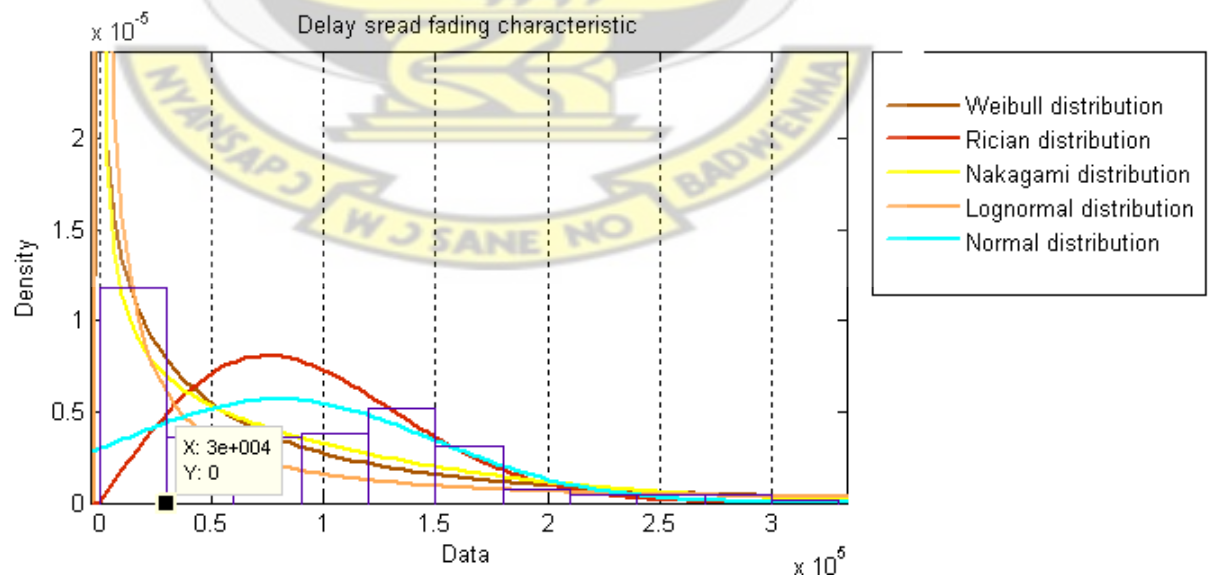


Figure 4. 12: Delay spread profile characteristic

By computing the mean of the standard deviation (std) on Rx, and calculating the standard deviation of the measurement spread, we obtained the shadowing and the path loss exponent of the environment respectively in Table 4.1, 4.3, 4.5, 4.7, 4.9 and 4.11

Table 4. 1: Statistics of measured received power in environment B (Near field)

Distance/m	Standard deviation/dB	Mean/dBm	Median/dBm	Difference/dB
50	5.13	-71.23	-70.00	1.23
100	7.71	-72.91	-74.00	1.09
150	2.74	-78.15	-78.00	0.15
200	3.70	-74.83	-75.00	0.17
250	6.74	-74.30	-73.00	1.30
300	9.47	-58.89	-57.00	1.89

In Table 4.1, the path loss exponent is 2.535 which is higher than that of free space. The shadowing effect in the near field of environment is 5.915dB. The median values of the received power signal and the mean values differ by 0.972 dB. The Table 4.2 gives comparison between two different linear fitting methods. The aim is to derive the slope of the graph which in turn is the true representation of the path loss exponent. It is then observed that the second column (the data of received power measurement has been normalized) gives a rough idea of the path loss exponent (p1). Figure 4.13 shows its corresponding autocorrelation of shadowing.

Table 4. 2 Statistics linear fitting (near field environment B)

Linear model Poly1: $f(x) = p1*x + p2$ Coefficients (with 95% confidence bounds): p1 = 6.948 (-23.86, 37.76) p2 = -65.99 (-92.66, -39.32) Goodness of fit: SSE: 203.9 R-square: 0.08926 Adjusted R-square: -0.1384 RMSE: 7.141	Linear model Poly1: $f(x) = p1*x + p2$ where x is normalized by mean -0.8248 and std 0.2878 Coefficients (with 95% confidence bounds): p1 = 1.999 (-6.867, 10.87) p2 = -71.72 (-79.81, -63.62) Goodness of fit: SSE: 203.9 R-square: 0.08926 Adjusted R-square: -0.1384 RMSE: 7.141
---	--

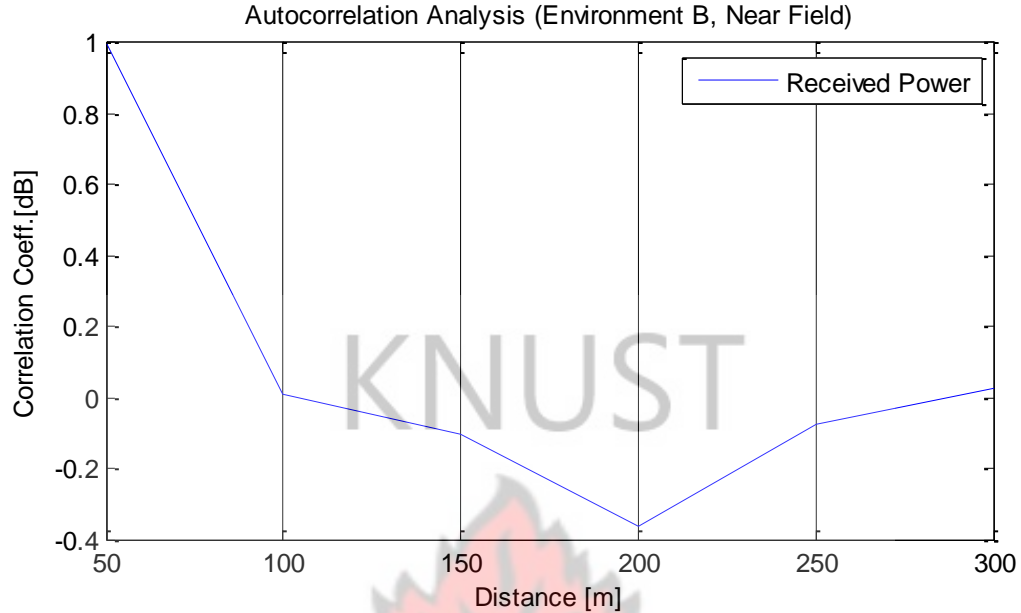


Figure 4. 13 Autocorrelation of shadowing in near field (environment B)

Table 4. 3: Statistics of measured received power in environment B (far field)

Distance/m	Standard deviation/dB	Mean /dBm	Median/ dBm	Difference/dB
500	4.48	-76.40	-76.00	0.64
600	5.52	-73.58	-75.00	1.42
700	5.65	-68.21	-69.00	0.79
800	3.54	-63.97	-64.00	0.03
900	8.56	-72.27	-72.00	0.27
1000	4.97	-75.03	-75.00	0.03

In Table 4.3, the path loss exponent is which 1.705 is less than that of free space. The shadowing effect in the far field of environment is 5.453dB which gives indication that the level of obstruction is higher compared to that of the near field of environment B. The median values of the received power signal and the mean values differ by 0.53.dB and Figure 4.14 shows its corresponding autocorrelation of shadowing.

Table 4. 4 Statistics linear fitting (far field environment B)

<p>Linear model Poly1: $f(x) = p1 * x + p2$ Coefficients (with 95% confidence bounds): $p1 = 10.61 (-45.14, 66.35)$ $p2 = -70.13 (-79.65, -60.6)$</p> <p>Goodness of fit: SSE: 101.8 R-square: 0.06521 Adjusted R-square: -0.1685 RMSE: 5.044</p>	<p>Linear model Poly1: $f(x) = p1 * x + p2$ where x is normalized by mean - 0.1367 and std 0.1124 Coefficients (with 95% confidence bounds): $p1 = 1.192 (-5.072, 7.455)$ $p2 = -71.58 (-77.29, -65.86)$</p> <p>Goodness of fit: SSE: 101.8 R-square: 0.06521 Adjusted R-square: -0.1685 RMSE: 5.044</p>
--	--

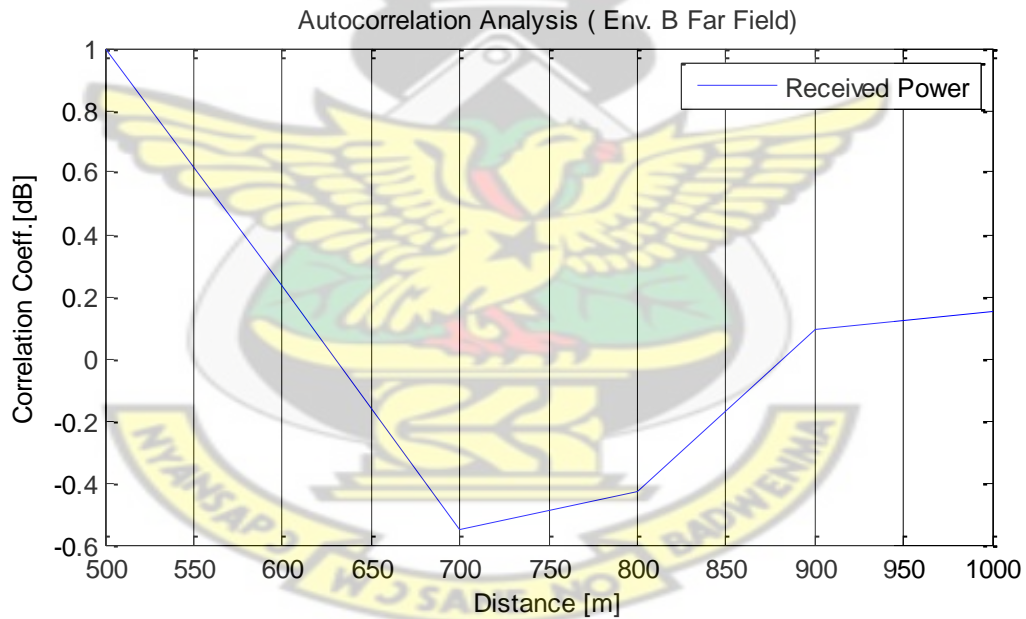


Figure 4. 14 Autocorrelation of shadowing in far field (environment B)

Table 4. 5: Statistics on measured received (Rx) power (near field environment C)

Distance/m	Standard deviation /dB	Mean /dBm	Median /dBm	Difference/dB
50	10.88	-70.56	-69.00	1.56
100	5.52	-78.30	-79.50	1.20
150	2.36	-82.08	-82.00	0.08
200	1.90	-83.57	-83.00	0.57
250	1.79	-78.20	-79.00	1.20
300	5.24	-80.47	-81.50	1.17

In Table 4.5, the path loss exponent is 1.857 representing the rate of decay in the received power attenuated along the transmitter-receiver separation distance but it is less than that of free space. The shadowing effect in the near field of Legon is 3.362dB but the standard deviation of 10.88dB is ignored because it is too high at the near field or it can be seen as aberration measurement. The median values of the received power signal and the mean values also differ by 0.96dB, this can be used to quantify statistical fading distribution. Consequently, in Rayleigh fading distribution the mean and its median differ by 0.55dB as in (Rao, 2010) therefore, the observed fading distribution may not be said to follow Rayleigh fading distribution and the corresponding autocorrelation of shadowing is shown in Figure 4.15.

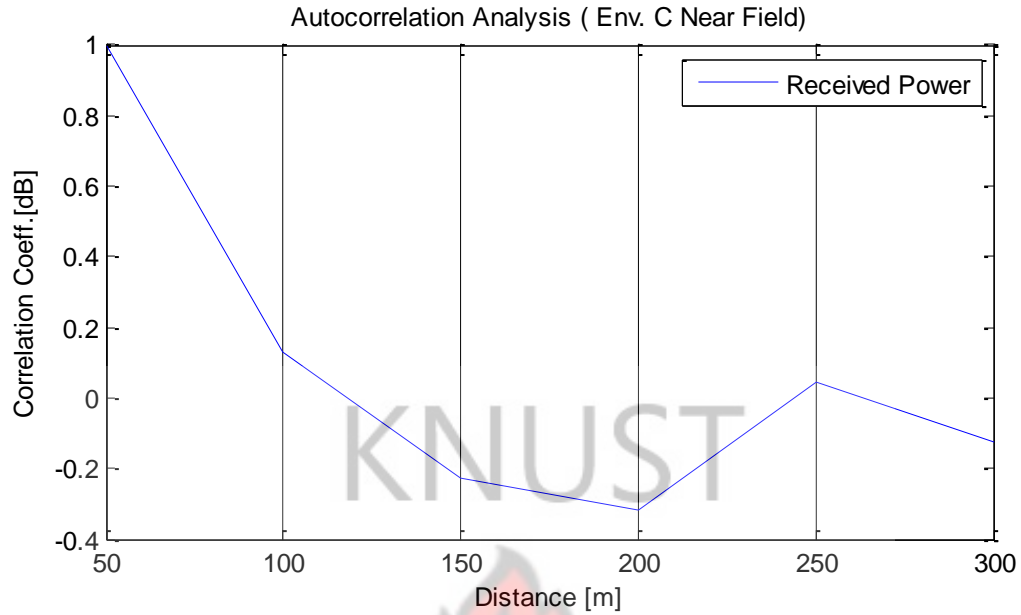


Figure 4. 15 Autocorrelation of shadowing in near field (environment C)

Table 4. 6 Statistics of measured received power (Far field environment C)

Distance/m	Standard deviation/dB	Mean/dBm	Median/dBm	Difference/dB
500	5.74	-78.46	-80.00	1.54
600	3.27	-82.28	-83.00	0.72
700	8.92	-77.78	-80.00	2.22
800	5.29	-79.17	-81.00	1.83
900	6.88	-75.54	-77.50	1.96
1000	6.98	-76.99	-77.50	0.55

In Table 4.6, the path loss exponent is 1.902 which is lower than that of free space but then it may be argued that the propagation effect is as in guided wave transmission media because the medium is lossless. The shadowing effect in the far field of Legon is 6.18dB which gives indication that the level of obstruction is higher compared to the near field of the same environment. The median values of the received power signal and the mean

values differ by 1.47.dB and its corresponding autocorrelation of shadowing is shown in Figure 4.16.

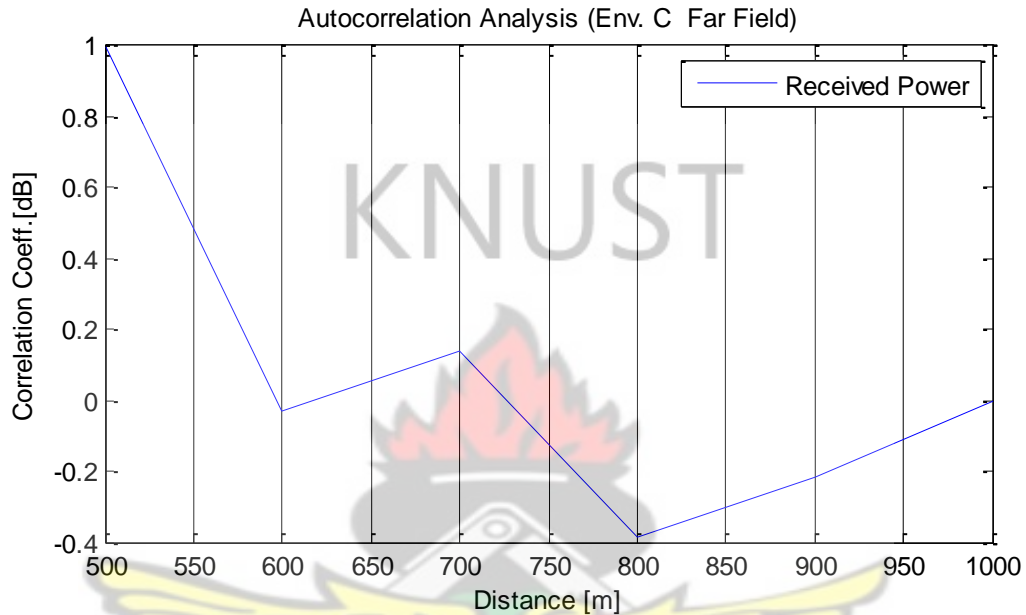


Figure 4. 16: Autocorrelation of shadowing in environment B (Far - field)

Table 4. 7 Statistics of measured received power in the near field (Environment D)

Distanc/m	Standard deviation/dB	Mean/dBm	Median/dBm	Difference/dB
50	5.50	-71.23	-70.00	1.23
100	7.60	-72.91	-74.00	1.09
150	2.64	-78.15	-78.00	0.15
200	2.60	-74.83	-75.00	0.17
250	2.65	-50.25	-50.50	0.25
300	5.22	-58.89	-52.00	1.34

In Table 4.7, the path loss exponent is 2.074 which is equal to that of free space. The shadowing effect in the far field of environment is 4.368dB. The median values of the received power signal and the mean values differ by 0.705dB, and Figure 4.17 shows its corresponding autocorrelation of shadowing.

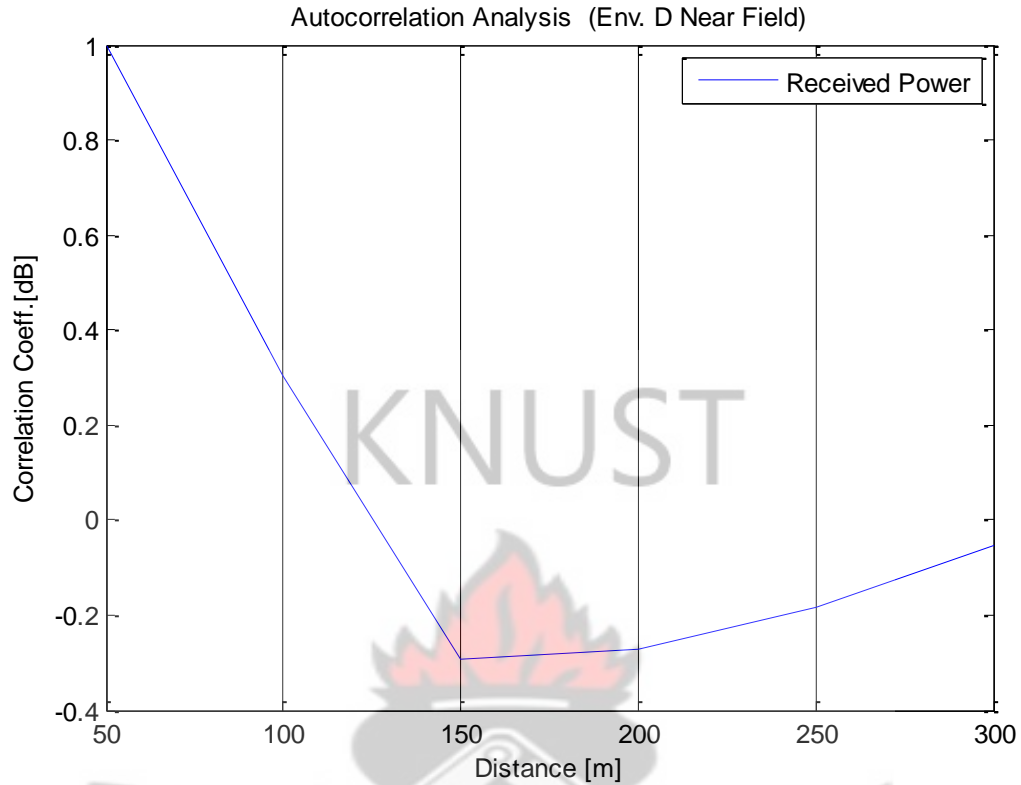


Figure 4. 17 Autocorrelation of shadowing in environment D (Near - Field)

Table 4. 8 Statistics of measured received power in the far field (**Environment D**)

Distance/m	Standard deviation/dB	Mean/dBm	Median/dBm	Difference/dB
500	5.11	-59.24	-57.50	1.74
600	4.02	-67.37	-67.50	0.13
700	4.09	-66.66	-66.00	0.66
800	4.13	-67.08	-67.00	0.08
900	4.13	-72.08	-71.00	1.08
1000	6.65	-70.63	-71.00	0.27

Table 4.8 the path loss exponent is 1.044 which is lower to that of free space. The shadowing effect in the far field of environment is 4.688dB which gives indication that the level of obstruction is less compared to that of the near field of environment B. The

median values of the received power signal and the mean values differ by 0.66dB and its respective autocorrelation of shadowing is shown Figure 4.18

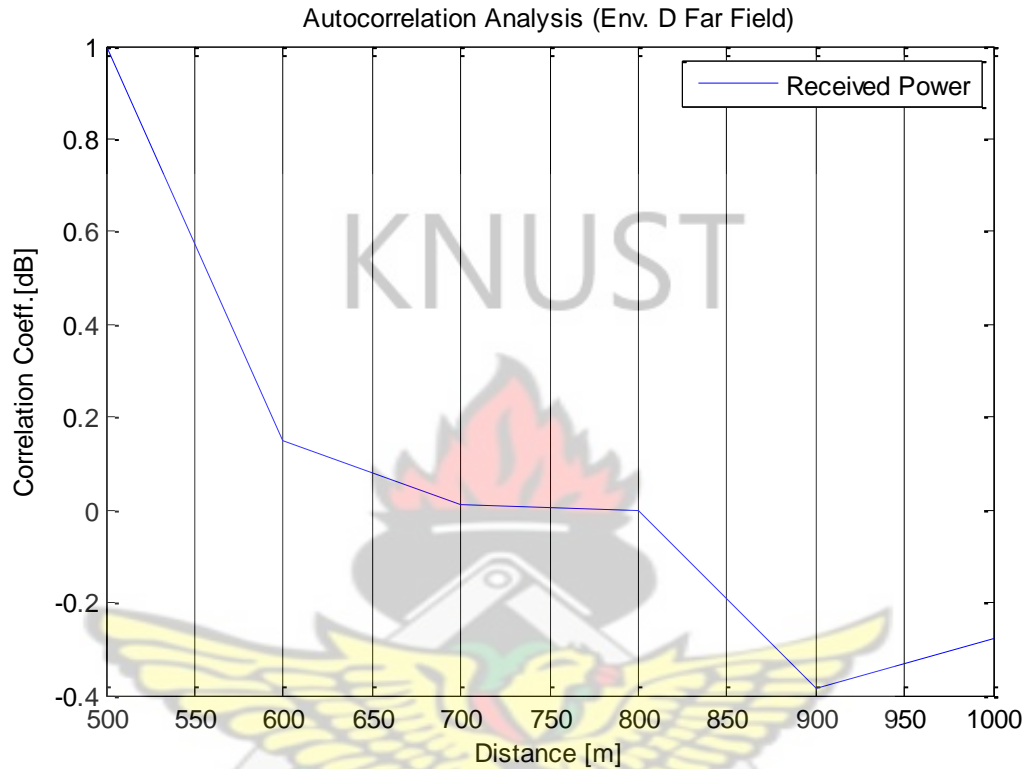


Figure 4. 18: Autocorrelation of shadowing in environment D (far - field)

From Table 4.1,4.3, 4.5, 4.7,4.9.and 4.11 It is observed that different path loss exponents values are obtained in both near field and far field because of the materials used for the construction of the buildings ,trees, human beings and the size of the environment as observed by (Nam H. , 2008) using indoor measurements. The standard deviation of shadowing is in the ranges from 4.368dB to 6.180dB.

Table 4.9 statistics on environment D using data fitting tool

Near field	Far field
Linear model Poly1:	Linear model Poly1:
$f(x) = p1*x + p2$	$f(x) = p1*x + p2$
Coefficients (with 95% confidence bounds):	where x is normalized by mean -0.1367 and std 0.1124
p1 = -35.03 (-60.83, -9.226)	Coefficients (with 95% confidence bounds):
p2 = -71.97 (-76.38, -67.56)	p1 = -3.936 (-6.835, -1.037)
Goodness of fit:	p2 = -67.18 (-69.82, -64.53)
SSE: 21.81	Goodness of fit:
R-square: 0.7803	SSE: 21.81
Adjusted R-square: 0.7254	R-square: 0.7803
RMSE: 2.335	Adjusted R-square: 0.7254
	RMSE: 2.335

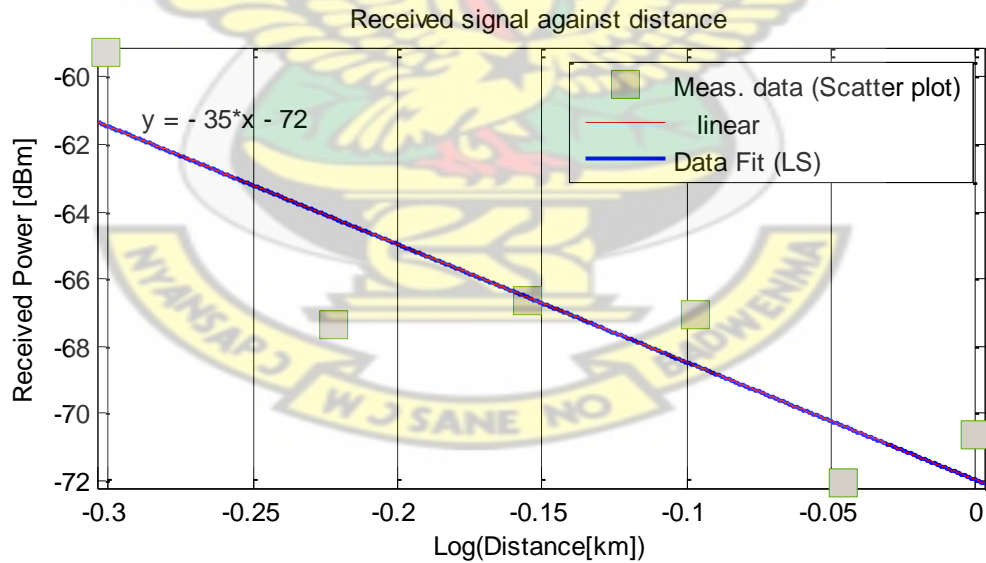


Figure 4. 19: Data fitting plot (near field environment D)

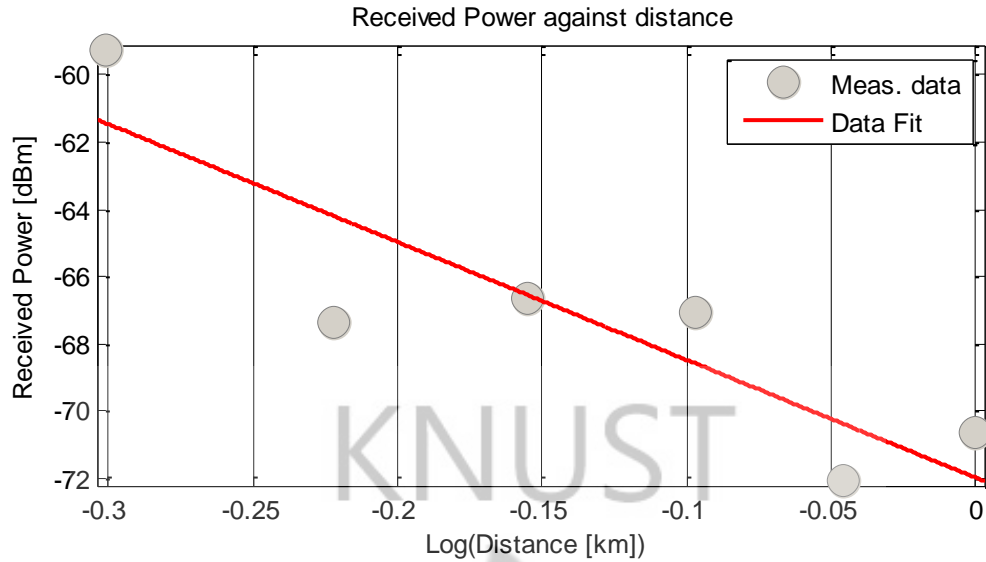


Figure 4. 20 Data fitting plot (far field environment D)

A comparison is made between the calculated one and the data fitting plot for environment D and it is observed that the path loss exponents are higher when data fitting tool is used than the calculated one.

4.6. Delay spread optimization using least square algorithm

$$\text{Recall: } E[Rx_i, Rx_i - \Delta Rx] = \sigma^2 * \exp\left(-\frac{|\Delta Rx|}{\Delta d}\right) \quad (4.1)$$

The following curves show the exponential decay nature of the delay spread as expressed by equation (4.1) where σ^2 is the variance ΔRx is the variation in the received power signal and Δd is the variation in the transmitter- receiver separation distance. In Figure 4.26, the plot of the delay spread using equation 4.1 is then shown.

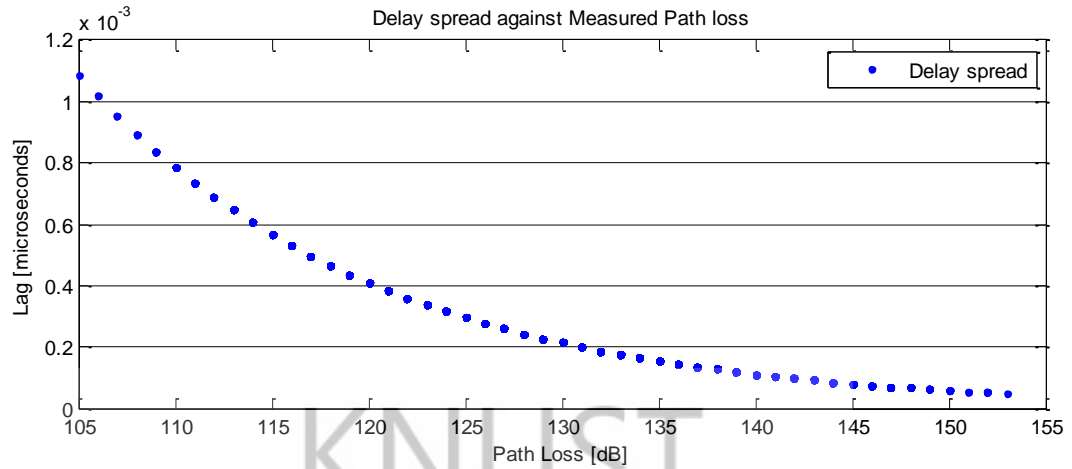


Figure 4. 21: The theoretical delay spread

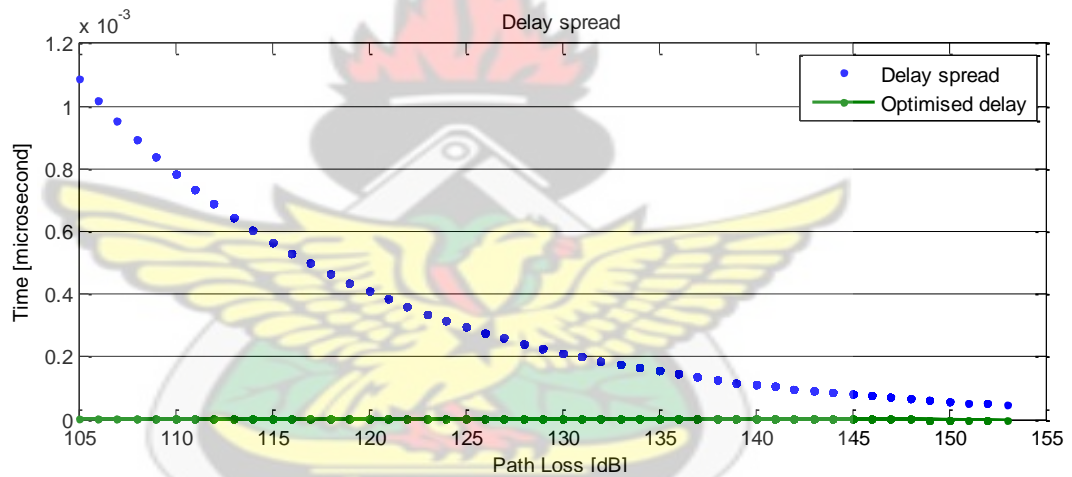


Figure 4. 22: The optimized delay spread

In Figure 4.21, it was observed that the delay spread is high. The green plot in Figure 4.22 is the optimized delay spread. This plot is obtained by considering the modified k value using the least square algorithm. The mean value of k is 0.500 for the macrocell; however its value for the microcell is 0.065. It is seen that with the obtained k value the delay spread can be highly optimized.

4.7. The Weibull Parameters in Ghana mobile environment

In Figure 4.23 environments B, C and D may all be seen as described by Weibull fading distribution.

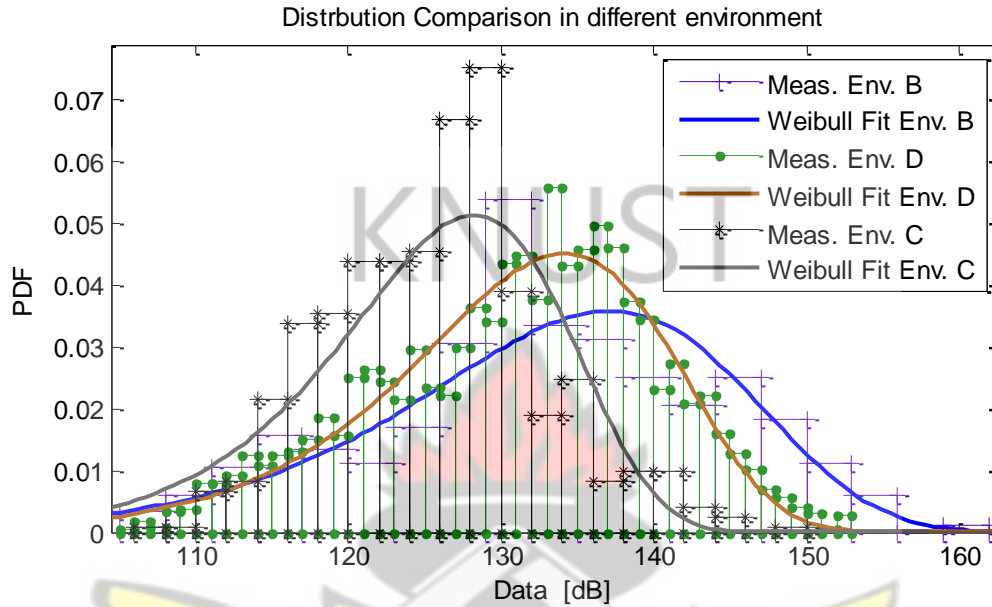


Figure 4.23 Weibull distribution comparisons in different environments

Their characteristic is shown in Table 4.9.

Table 4.9: Derived of weibull's fading parameters

Environment B	Environment C	Environment D
Log likelihood: -133363	Log likelihood: -2183.87	Log likelihood: -2086.03
Domain: $0 < y < \text{Inf}$	Domain: $0 < y < \text{Inf}$	Domain: $0 < y < \text{Inf}$
Mean: 130.437	Mean: 132.698	Mean: 124.897
Variance: 94.9564	Variance: 146.392	Variance: 74.101
Parameter Estimate Std. Err.	Parameter Estimate Std. Err.	Parameter Estimate Std. Err.
a 134.69 0.044988	a 137.931 0.456684	a 128.664 0.309495
b 16.481 0.0657705	b 13.3891 0.425608	b 17.9185 0.515055
Estimated covariance of parameter estimates:	Estimated covariance of parameter estimates:	Estimated covariance of parameter estimates:
a b	a b	a b
a 0.00202392 0.000951551	a 0.20856 0.0631941	a 0.0957869 0.0532878
b 0.000951551 0.00432576	b 0.0631941 0.181142	b 0.0532878 0.265281

The results in **Table 4.9** are being used to obtain the optimised parameters in Weibull. The Weibull fading model in the study environment of Ghana, as shown in Figure 4.24 to 4.26 is being compared with the measured data in Environment B, C and D respectively.

Using a function in Matlab software that gives the PDF of Weibull, of a random variable X , where the scale and shape parameters \mathbf{a} , and \mathbf{b} respectively are unknown.

```
Y = wblpdf(X,a,b) % weibull distribution
```

Using the distribution fitting tools in Matlab software, \mathbf{a} and \mathbf{b} are computed.

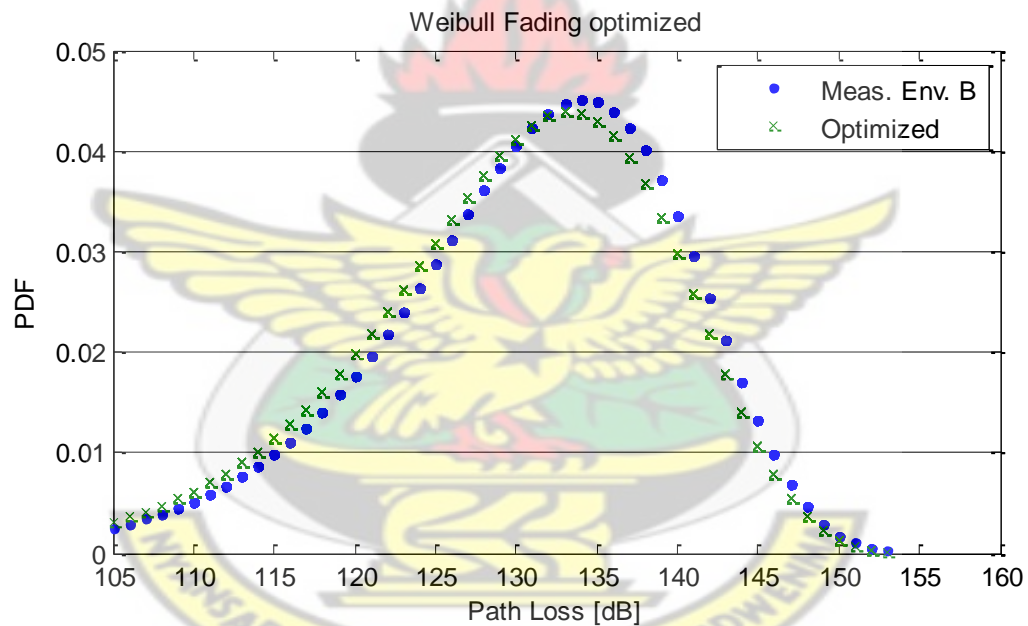


Figure 4. 24: Optimized Weibull fading model (Env. B)

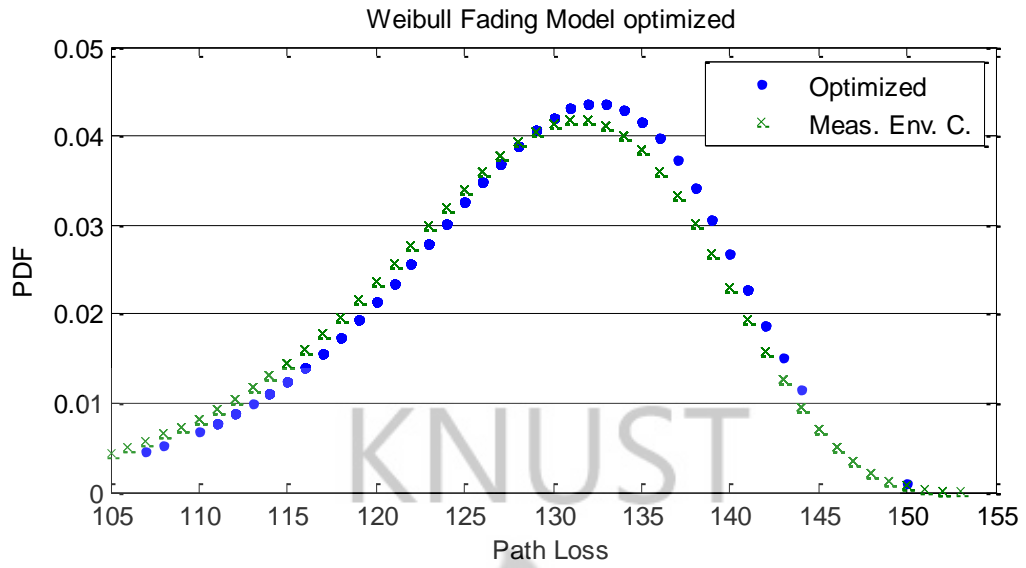


Figure 4. 25: Optimized Weibull fading model (Env. C)

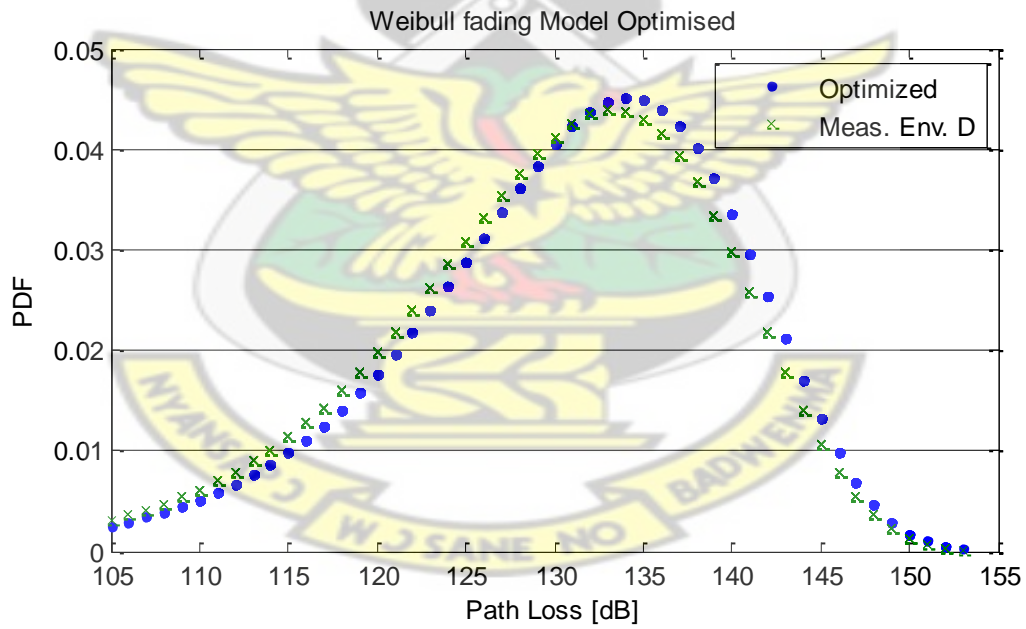


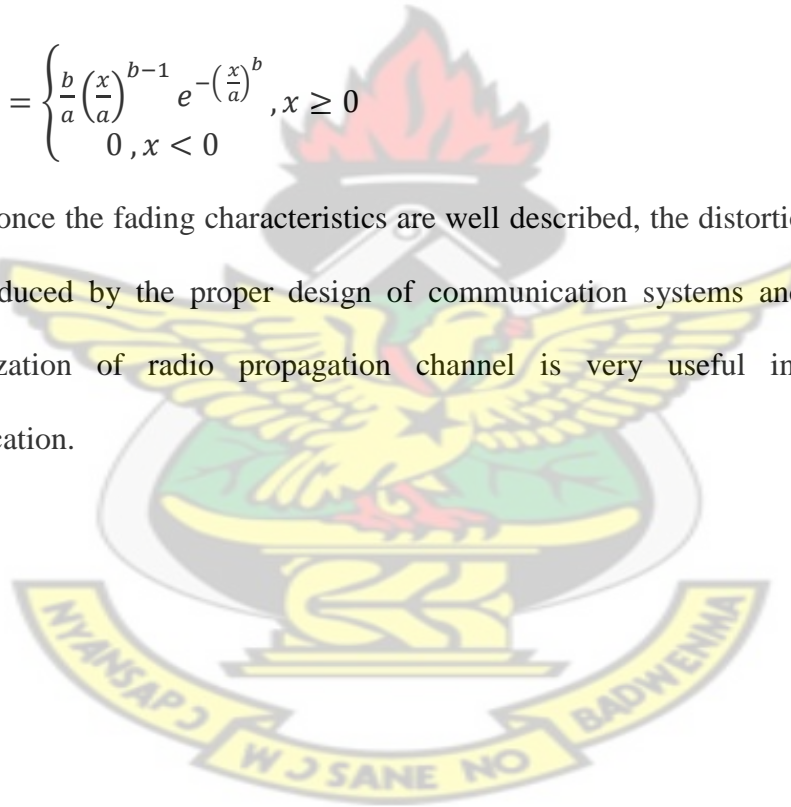
Figure 4. 26: Optimized Weibull fading model (Env. D)

The optimised parameters are obtained using the mean of the parameters in Environments. B, C, D as shown in the Table.4.9.

The Weibull fading distribution is described by the scale parameter and shape parameter. The mean scale parameter (a) and the mean shape parameter (b) for the environments are 133.76 and 15.93 respectively where a very close agreement is been achieved in the three environment. Therefore Weibull fading distribution in Ghana can be written as in Equation 4.2.

$$f(x, a, b) = \begin{cases} \frac{b}{a} \left(\frac{x}{a}\right)^{b-1} e^{-\left(\frac{x}{a}\right)^b}, & x \geq 0 \\ 0, & x < 0 \end{cases} \quad (4.2)$$

however, once the fading characteristics are well described, the distortion by the channel can be reduced by the proper design of communication systems and thus a detailed characterization of radio propagation channel is very useful in the design of communication.



CHAPTER FIVE

CONCLUSION AND RECOMMENDATIONS

In this study, the received power signal is obtained by using the drive-test system. The study investigates the fading distribution on received power measurement. The analysis of the received power envelope is done by using distribution fitting tool for the small-scale fading and curve fitting tool for the large-scale fading in Matlab software 7.5.0(R2007b).

The results show that the Weibull fading distribution is found to give the best description of fading experienced in Ghana. On the other hand, Rician distribution, Nakagami-m distribution and lognormal distribution have less agreement with the measured data while Rayleigh fading distribution also has much less agreement with measured data. The result of analysis on large-scale fading shows that the large scale fading tends to describe the terrain profile of the environment and does depend on the distance.

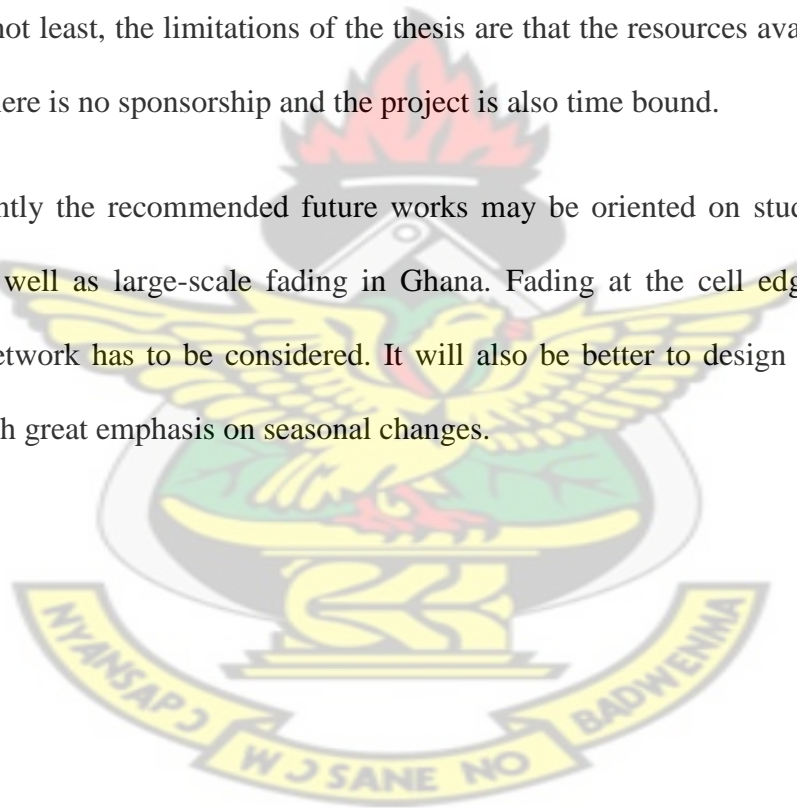
Moreover the root-mean square (rms) delay spread cannot be characterised by both Rayleigh and Rician distributions. A clear dependence between the root mean square (rms) delay spread values and the transmitter-receiver separation distance is observed.

The Weibull fading distribution is described by the scale parameter and shape parameter. The obtained mean scale parameter and the mean shape parameter for the environment considered are 133.76 and 15.93 respectively. However, once the fading characteristics are well described, the distortion by the channel can be reduced by the proper design of

communication systems and thus a detailed characterization of radio propagation channel is very useful in the design of communication systems. Small-scale fading studies help us to know which type of modulation scheme can be used for a particular environment. Furthermore determining the relationship between the received power signal and the distance helps us in ranging and positioning technologies in wireless sensor networks (Xu et al, 2010). Different path loss exponents are obtained in both near field and far field. The standard deviation of shadowing falls in the ranges of 4.368dB to 6.180dB.

Last but not least, the limitations of the thesis are that the resources available are limited because there is no sponsorship and the project is also time bound.

Consequently the recommended future works may be oriented on studying small-scale fading as well as large-scale fading in Ghana. Fading at the cell edge in the case of cellular network has to be considered. It will also be better to design fading model for Ghana with great emphasis on seasonal changes.



REFERENCES

- (2009). Retrieved April 5, 2011, from antenna-theory: www.antenna-theory.com
- (2010, march 11). Retrieved march 20, 2011, from radio-electronic: www.radio-electronic.com
- (2011). Retrieved MARCH 26, 2011, from experiment-resources: www.experiment-resources.com
- (2011). Retrieved March 26, 2011, from Statsoft: www.statsoft.com
- (2011). Retrieved March 20, 2011, from wiki. answer web site: wiki.answers.com
- (2011, january 7). Retrieved june 1, 2011, from wikipedia: www.wikipedia.com
- antenna-theory*. (2011). Retrieved April 5, 2011, from antenna-theory: www.antenna-theory.com/basics/fieldRegions.php
- Athanasiadou et al. (2000). *A microcellular ray-tracing propagation model and evaluation of its narrow-band and wide-band*. Harlow: IEEE.
- Ayadi et al. (2005). Ray tracing model for urban micro-cellular system at 1800MHz band. *Third International conference on systems. III*. Tunis: IEEE.
- Baltizis, K. B. (2010, April). Closed-Form Description of Microwave Signal Attenuation in Cellular Systems. *Radioengineering, Vol. 19*, pp. 11-16.
- Belloni, F. (2004). Fading models. 1-3.
- Bultitude et al. (1988). Propagation considerations for the design of an indoor broadband communications systems at EHF. *47 (1)*, 235-245.
- chan, I. (2010). understanding the effect of environment facts link quality for on-board communication.
- Chugg, K. (1999, August). *Mobile communication systems*.
- Collonge et al. (2003). Wideband and Dynamic characterization of 60GHz indoor radio propagation- future home WLAN architectures. *58*, 417-447.
- Cox, D. C. (1973, November). 910 MHz Urban Mobile Radio Propagation: Multipath Characteristics in New York City. *IEEE Trans. Communication*, p. Vol. 21.
- D. C. Cox. (1972, September). Delay Doppler Characteristic of Multiple Propagation at 910MHz in a Suburban Mobile Radio Environment. *IEEE Trans. Antennas Propagation*, p. Vol. 10.

- Daniels, s. A. (2010, August 11). factors that affect signal strength. *EzineArticles* .
- Dotche, K. A. (2011, January 27). *Sensitivity of Received Power in Antenna Downtilt in Mobile Cluttered Environments*. Retrieved from www.knust.edu.gh.
- Edwards, R., & Durkin, J. (1969). Computer Prediction of Service Area for VHF Mobile Radio Networks. *Proceeding of the IEEE, Vol. 116, no. 9* , 11493-1500.
- Feuerstein et al. (1994, August). Path Loss, Delay Spread, and Outage model as Function of Antenna Height for communication System Design. *IEEE Transaction on Vehicular Technology, Vol. VT-43, No. 3* , pp. 487-498.
- Forkel et al. (2008). Generation of two-dimensional correlated shadowing for mobile radio network simulation.
- Goldsmith, A. (2005). *wireless communications*. Cambridge university press.
- Graziano, V. (1978). Propagation correlation at 900MHz. *IEEE transsaction on vehicular technology* , 4, 182-189.
- Gudmundson, M. (1997). Correlation model for shadow fading in mobile radio systems. *electronics letters* , 27, 2145-2146.
- Gudmundson, M. (1991, November). Correlation Model for Shadow Fading in Mobile Radio Systems. *Electron. Lett.* , pp. 2145-2146.
- Hashemi ,K ; Tholl, D. (1994). statistical modeling and simulation of the RMS delay spread of indoor radio propagation channels. *IEEE transactions on vehicular Technology* , 43 (1).
- Hata, M. (1980, August). Empirical Formula for Propagation Loss in Land Mobile Radio Services. *IEEE Transactions on Vehicular Technology, Vol. VT-29, no 3* , pp. 317-325.
- Hong A, Thomae R.S. (2009). Experimental study on the impact of the base station height on the channel parameters. *International ITG Workshop on smart Antennas*. Berlin.
- Jalden et al. (2005). *Inter and Intra site correlation of large scale parameters from macro cellular measurements at 1800MHz*. Stockholm: Royal institute of Technology.
- Jalden et al. (2006). *Correlation properties of large scale fading based on indoor measurements*. stockholm and Illmenau: Royal institute of technology.
- Johnson, D. (2009, june 9). line-of-sight transmission.
- Krievs, R. (2004). Empiric characteristics of fading mobile communication channels. *Elektronika Ir Elektrtechnka* , 52-55.

Lempiainen, J., & Manninen, M. (2003). *UMTS Radio Network Planning Optimization and QoS Management*. Dordrecht, Netherland: Kluwer Academic.

Longley, A., & Rice, P. (1968). Prediction of Tropospheric Radio Transmission Loss over Irregular Terrain. *Tech Rep. ERL 79-ITS, ESSA Technical Report* .

Manninen, J. L. (2003). *UMTS Radio Network Planning Optimization and QoS Management*. Dordrecht, Netherland: Kluwer Academic.

Nam, H. (2008). *statistical analysis of indoor radio propagation channel characteristics at 60GHz*. Austin: The university of Texas.

Nam, H. (2008). *statistical analysis of indoor radio propagation channel characteristics at 60GHz*. Austin: The university of Texas.

Nikookar H, Hashemi H,. (2008). statistical modeling of signalamplitude fading of indoor radio propagation channels. *IEEE Xplore* (pp. 84-88). Teheran: Amirkabir university of technology.

Nikookar, Homayoun; Hashemi, Homayoun. (2008). *Sttistical modeling of signal amplitude fading of indoor radio propagation channels*. electrical engineering. Teheran: Amirkabir university of technology and Sharif university of technology.

Oestges et al., (2009). *experimental characterization and modeling of outdoor-to-indoor and indoor-to-indoor distributed channels*. Braunschweig: European cooperation in the field of scientific and technical research.

Ohashi M, Shiraki K. (1991). Correlation model for shadow fading in mobile radio systems. 27, 2145-2146.

Okumura et al. (1968). Field Strenght and its Variability in VHF and UHF Land Mobile Services. *Review Electrical Communication Laboratory, Vol. 16, no. 9-10* , 2935-2971.

Parsons, J. D. (1992). *The Mobile Radio Propagation Channel*. New york: Halted Press-Wiley and Sons, Second Edition.

Rao, M. R. (2010). *simulation modeling of statistical Nakagami-m fading channels*. punjab: Thapar university.

Rappaport et al. (1997). *Propagation and radio system design issues in mobile radio systems for the GloMo Project*. virginia polytechnic institute and state university, Bradley Department of electrical and computer engineering. virginia: Mobile and portable radion research group.

- Rappaport, T. S. (1996). *Wireless Communications: Principle and Practice*,. Upper Saddle River, New Jersey: Prentice Hall PTR, .
- Ren et al. (2010). Modeling and simulation of Rayleigh fading, path loss and shadowing fading for wireless mobile networks. *Elsevier* , 626-637.
- Rubio et al. (2007). Evaluation of Nakagami fading behaviour based on measurements in urban scenarios. *AEU -international journal of electronics and communication* , 61 (2), 135-138.
- Sagais et al. (2004). Error rates analysis of switched diversityreceivers in Weibull fading. *Electronic letters* , 40 (11).
- Santucci, F., & Granziosi, F. (2004). Joint Characterization of Outage Probability and Handover Performance in Cellular Mobile Networks. *IEEE Xplore* .
- Shepherd, N. H. (1977). Radio Wave Loss Deviation and Shadow Loss at 900 MHz. *IEEE Transactions On Vehicular Technology*, Vol. VT-26 No 4 , 309-313.
- Simon, M. K., & Alouini, M.-S. (2005). *Digital Communication Over Fading Channel*. : John Wiley & Sons, Ltd.
- Sklar, B. (1997, july). Rayleigh fading channels in mobile digital communication systems. 102-109.
- Smith et al. (1998). *Telecommunications Engineering*.
- StatSoft. (n.d.). *textbook/basics/statistics*. Retrieved March 26, 2011, from www.statsoft.com: www.statsoft.com
- Stefanovic et al. (2010). Second-order statistics of SC mscrodiversity system over gamma shadowed Nakagami-m fading channels. *Elsevier* , 413-418.
- Stefonovic et al. (2007). performance analysis of system with selection combining over correlated weibull fading channels in the presence of cochannel interference. *Elsevier* , 695-700.
- Sundstrom, M. (2006). *GSM off road propagation in the 900MHZ band at differenheights in a coniferous forest*. elctrical engineering. Stockholm: KTH.
- Tomasevic et al. (2010). Short-term fading simulation using artificial neural networks. *Elsevier* , 1-9.
- vali et al. (2010). Effect of rayleigh fading on non-coherent sequence synchronization for multi-user chaos based DS- CDMA. *Elsevier* , 1924-1939.

Walfisch, J., & Bertoni, H. (1988, October). A Theoretical Model of UHF Propagation in Urban Environments. *IEEE Transactions on Antennas and Propagation*, Vol. AP-36 , pp. 1788-1796.

Weitzen J, Lowe T. (2002). Measurement of angular and distance correlation properties of log-normal shadowing at 1900MHz and its application of PCS systems. *IEEE transaction on vehicular Technology* , 51.

wikipedia. (2011). Retrieved April 5, 2011, from wikipedia: www.wikipedia.com

wirelesscommunication. (2011). Retrieved April 5, 2011, from www.wirelesscommunication.com

Xia et al. (1993). Radio propagation characteristics for line-of-sight microcellular and personal communications. *IEEE transactions on antennas and propagation* , 40 (10).

Xiao et al. (2007). A cross-layer adaptive transmission scheme combined with SR-ARQ over correlated fading channels. *Elsevier* , 324-337.

Xu et al. (2010). Distance measurement model on RSSI in WSN. *wireless sensor network* , 606-611.

Xu, J ; Liu, W ; Lang, F ; Zhang, Y ; Wang, C. (2010, August 18). *scientific Research* , pp. 606-611.

Yip K.W, Ng T.S. (2000). A simulation model for Nakagami-m fading channels, $m=i$. *IEEE Transactions* , 48 (2), 214-221.

Zhang et al. (2008). *A novel spatial autocorrelation model of shadow fading in urban macro environment*. Beijing: Beijing university of posts and Telecommunications.

Zhang et al. (2008). *statistical analysis of 900MHz radio signal with autocorrelation properties*. Nankai: Nankai university.

Appendix A: Fading distribution and fitting algorithms

Lognormal distribution

Lognormal distribution is often mentioned in connection with fading over large area where nonstationarities in the channel are taken into consideration. (Nikookar, Homayoun: Hashemi, Homayoun, 2008)

The PDF of the lognormal distribution is given by

$$f(r) = \frac{1}{\sqrt{2\pi}\sigma r} \exp\left\{-\frac{(\ln r - \mu)^2}{2\sigma^2}\right\} u(r) \quad (\text{A1})$$

Equation (B1) shows that $\ln(r)$ has a normal distribution. This distribution has two parameters μ and σ .

Loess quadratic algorithm

The name "loess" is derived from the term "locally weighted scatter plot smooth," as it uses locally weighted linear regression to smooth data. The smoothing process is considered local because, like the moving average method, each smoothed value is determined by neighboring data points defined within the span. The process is weighted because a regression weight function is defined for the data points contained within the span. In addition to the regression weight function, you can use a robust weight function, which makes the process resistant to outliers. Finally, the method, loess uses a quadratic polynomial.

Least square algorithm

The Curve Fitting Toolbox uses the method of least squares when fitting data. Fitting requires a parametric model that relates the response data to the predictor data with one

or more coefficients. The result of the fitting process is an estimate of the model coefficients. To obtain the coefficient estimates, the least squares method minimizes the summed square of residuals. The residual for the i th data point r_i is defined as the difference between the observed response value y_i and the fitted response value \hat{y}_i and is identified as the error associated with the data

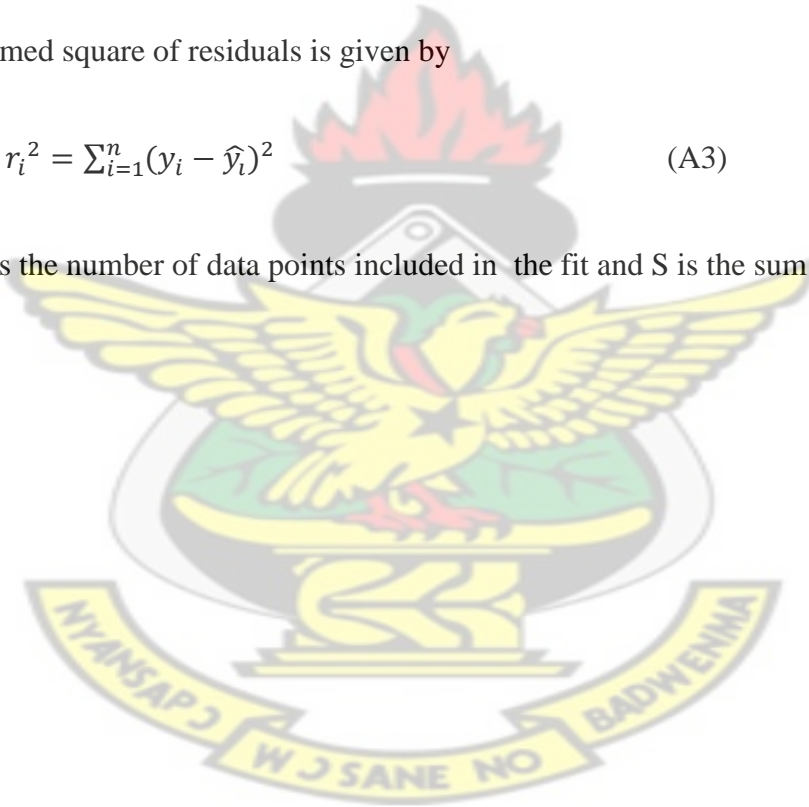
$$r_i = y_i - \hat{y}_i \quad (A2)$$

Residual = data - fit

The summed square of residuals is given by

$$S = \sum_{i=1}^n r_i^2 = \sum_{i=1}^n (y_i - \hat{y}_i)^2 \quad (A3)$$

where n is the number of data points included in the fit and S is the sum of squares error estimate.



Appendix B: Additional Figures

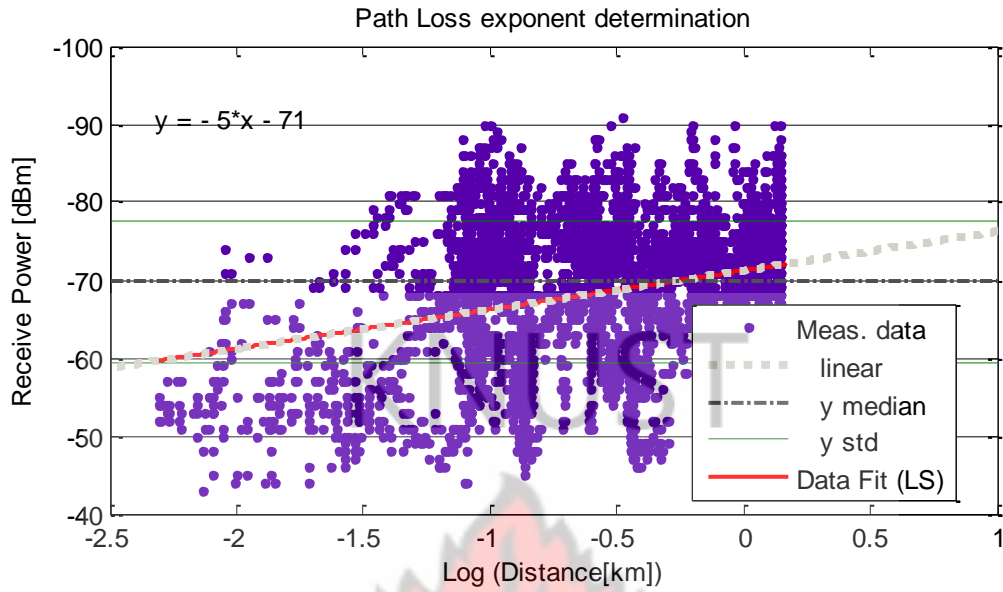


Figure B. 1: Path loss exponent determination

In Figure B.1 the linear fitting gives the same results as the least square fitting

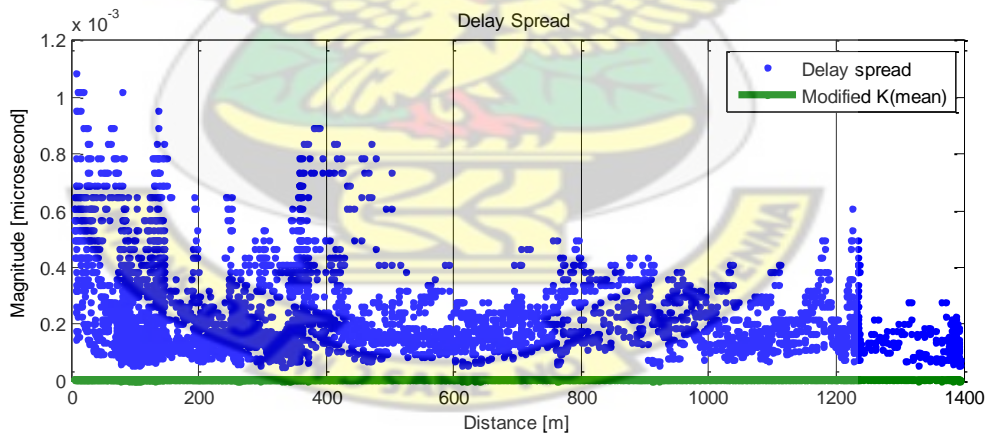


Figure B. 2: Comparison of delay spread scatter plot with the modified the K value

In Figure B.2, it was observed that the delay spread is high. The green plot in Figure B2 is the optimized delay spread. This plot is obtained by considering the modified k value using the least square algorithm. The mean value of k obtained is 0.500 for the macrocell; however its value for the microcell is 0.065.

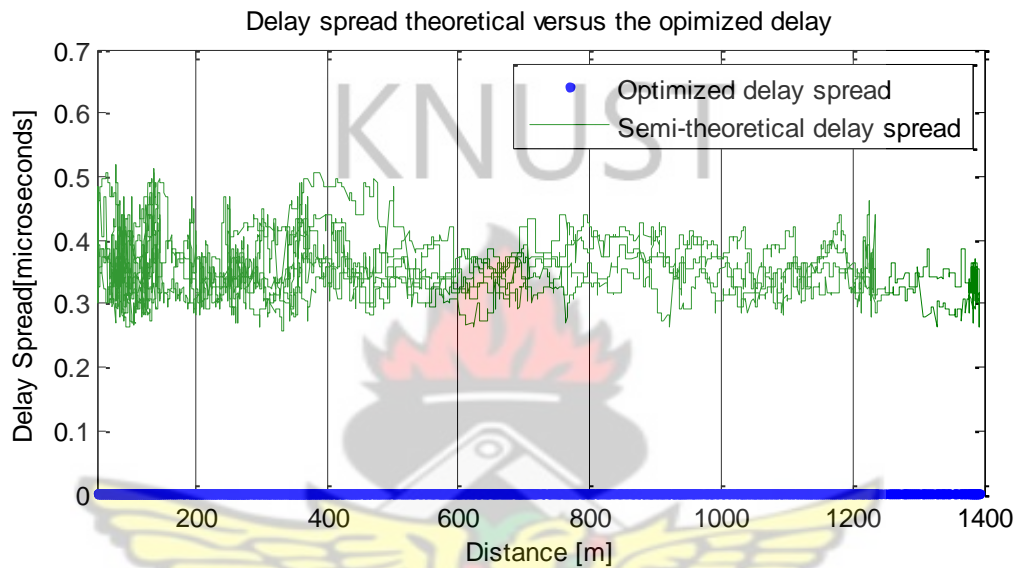


Figure B. 3: Comparison optimized delay spread and semi-theoretical delay spread.

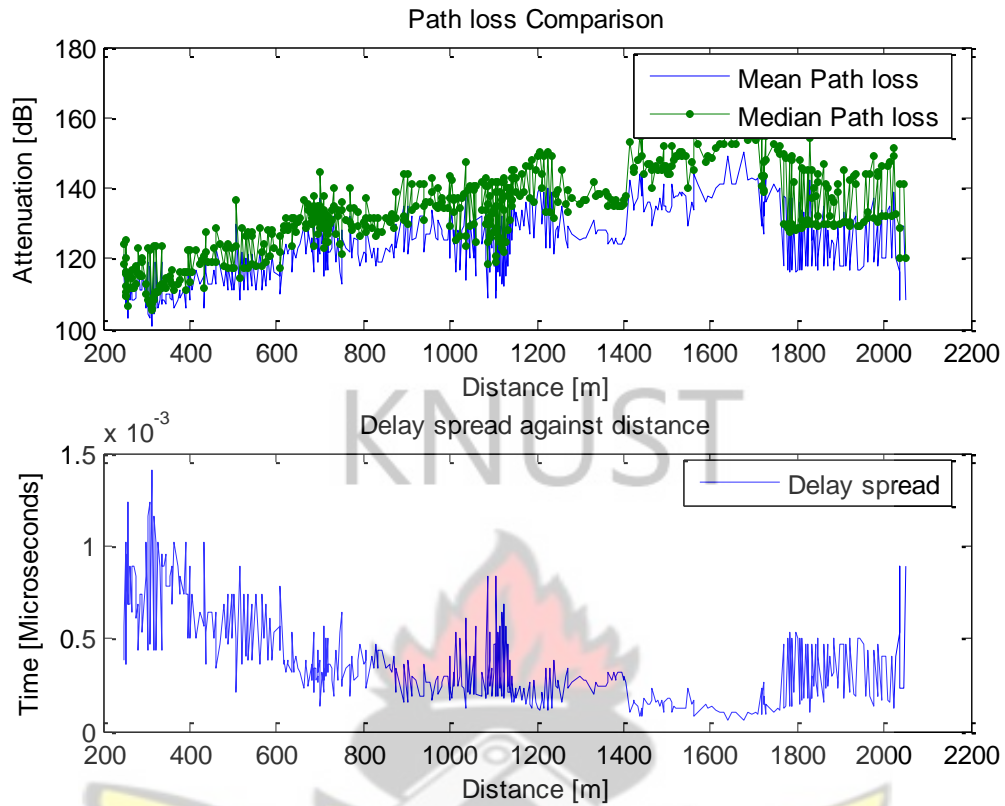


Figure B. 4: comparison of median and mean path loss

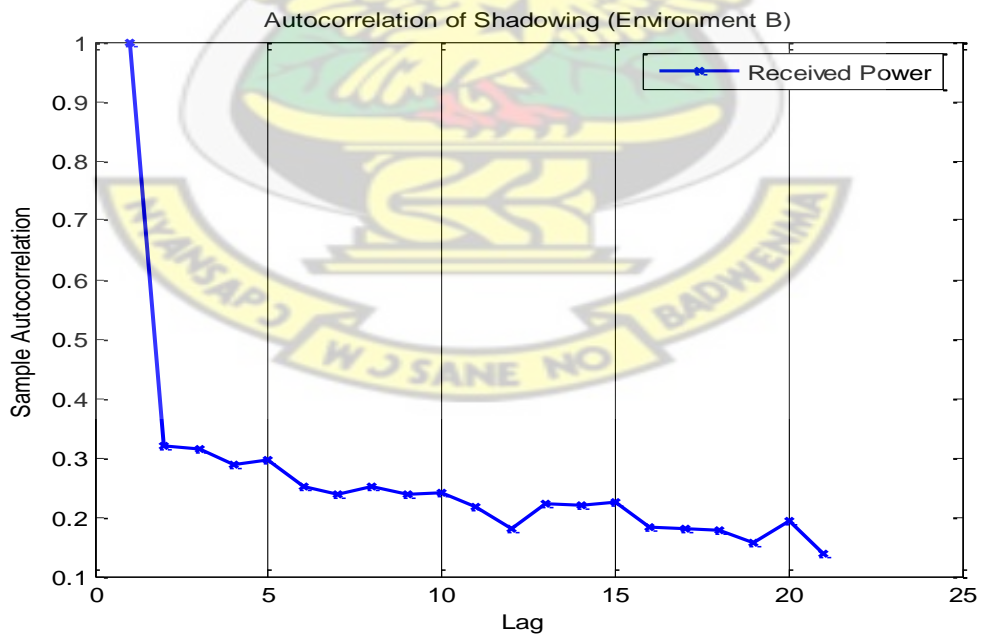


Figure B. 5: shadow autocorrelation on received power measurement profile

The shadow autocorrelation as shown in Figure B.5, is one side Gaussian noise extract. The noise is much high because the first lobe does not reach zero.

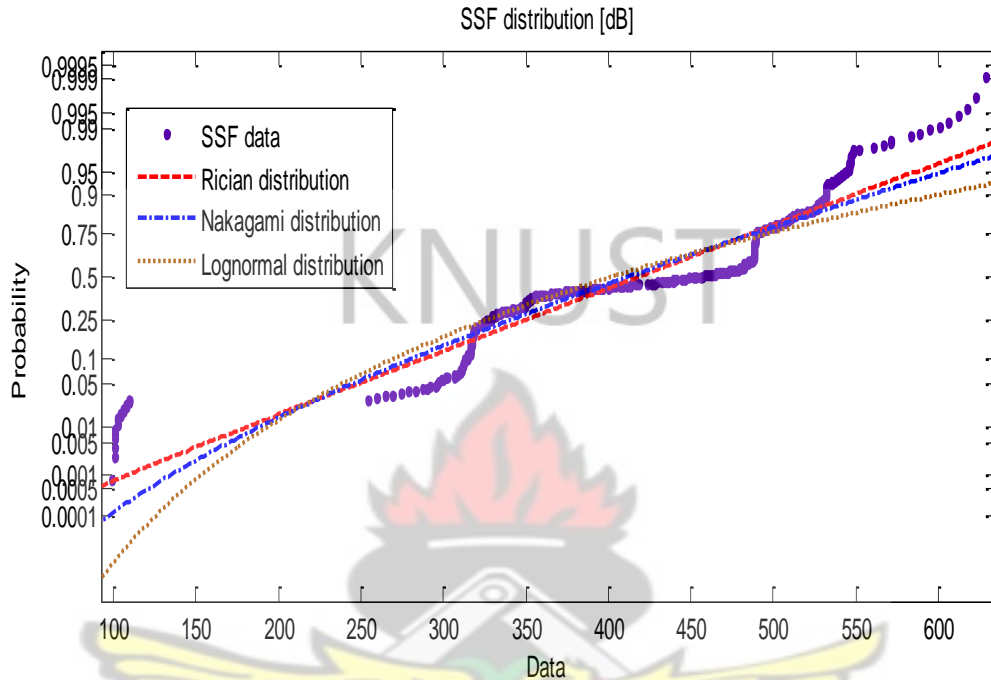


Figure B. 6: Probability plots analysis

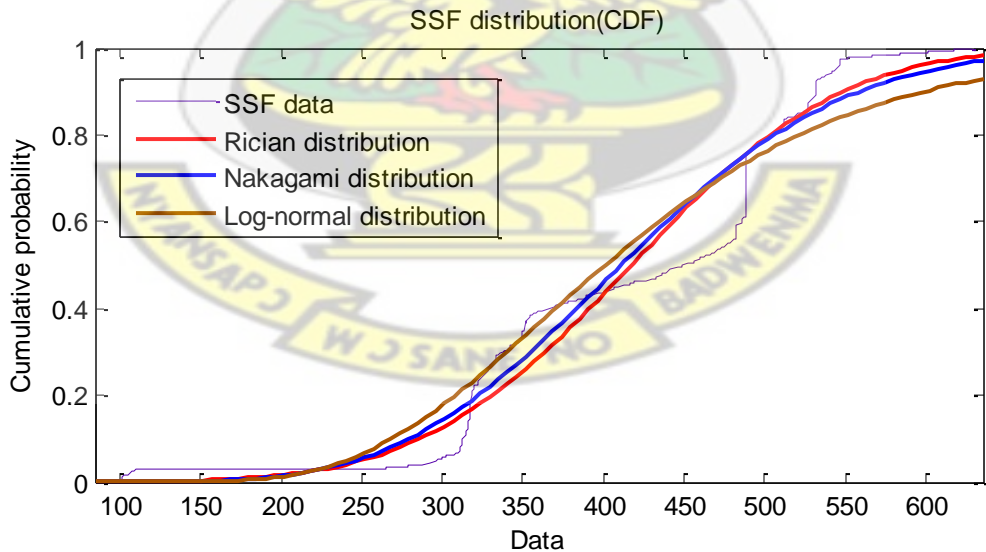


Figure B. 7: Cumulative probability plots analysis

In Figure B.6 - 7, plots analysis of cumulative density function (CDF) and probability function using line plot rather than histogram are used to fit the measured data and they

give little agreement with the measured data. The PDF gives better results as compared with CDF.

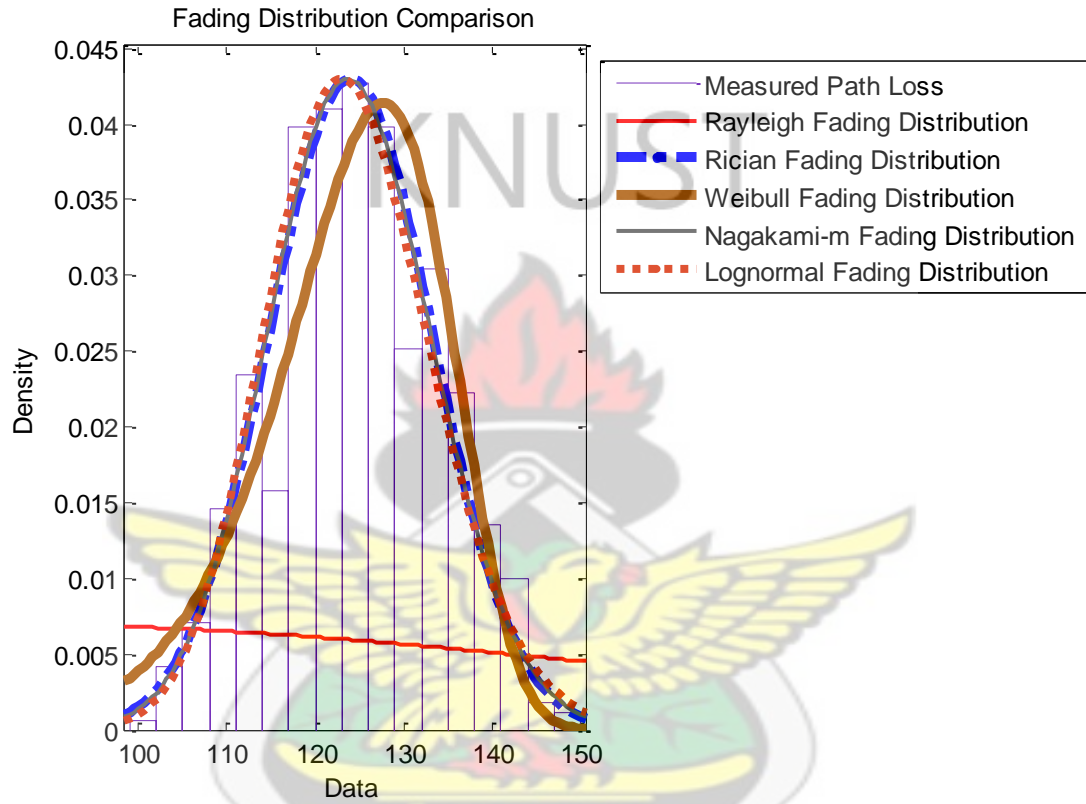


Figure B. 8: Fading distribution Comparison showing poor Rayleigh fading distribution with the measured data.

Appendix C: Additional Tables

In Table C1-4, are shown the process of computing the statistics on environment of Legon for instance.

Table C. 1 Legon Near field

Near field	Standard deviation (dB)	Mean (dBm)	Median (dBm)	Difference (dB)
N1	5.1	-62.2	-62	0.2
N2	4.3	-78.3	-79	0.7
N3	2.8	-82.1	-82	0.1
N4	1.8	-82.8	-82.5	0.3
N5	1.8	-82.8	-82.5	0.5
N6	2.8	-82.2	-81.5	0.7
N7	6.3	-79.1	-80	0.9
N8	11.6	-70.7	-69	1.7
N9	8.3	-70.9	-69	1.9
N10	2.5	-83	-83	0
N11	2.1	-83.1	-83	0.1
N12	3.6	-82.2	-82	0.2
N13	8.0	-78.3	-77.5	0.8
N14	8.0	-78.3	-77.5	0.8
N15	8.3	-77.6	-74	3.6
N16	2.0	-76.1	-77	0.9
N17	6.3	-70.5	-72	2.5
N18	3.1	-74.1	-75	0.9
N19	8.0	-78.3	-77.5	0.8
N20	8.0	-78.3	-77.5	0.8

Table C.1 shows the standard deviation, mean, median of the received power signal at the near field i.e for distances less than 300m (Legon).

Mean (of std on Rx) is 5.235 dB is the shadowing, and carrying the standard deviation 2.85 which indicates the path loss exponent of Legon.

Table C. 2; Far field Legon

Far field	Standard deviation(dB)	Mean(dBm)	Median(dBm)	Difference(dB)
F1	4.0	-73.2	-71.5	1.7
F2	3.8	-70.4	-70.5	0.1
F3	3.8	-70.4	-70.5	0.1
F4	4.2	-71	-69.5	1.5
F5	4.7	-72.2	-70	2.2
F6	4.4	-73.7	-74	0.3
F7	8.0	-71.9	-71.5	0.4
F8	4.1	-73.6	-74	0.4
F9	1.2	-81.3	-81.5	0.2
F10	0.8	-82.5	-82	0.5
F11	0.8	-83	-83	0
F12	1.1	-82.7	-83	0.3
F13	5.5	-79.3	-81.5	2.2
F14	5.5	-79.3	-81.5	2.2
F15	4.2	-71.5	-70	1.5
F16	4.5	-76.9	-76.5	0.4
F17	1.3	-77.7	-78	0.3
F18	1.5	-82.5	-83	0.5
F19	3.6	-84.3	-85	0.7
F20	5.1	-80	-80	0

Table C.2 shows the standard deviation, mean, median for the received power signal at the far field i.e. for distances greater than 300m (legon).

